

**EMISSION GUIDED RADIATION THERAPY: A  
FEASIBILITY STUDY**

A Thesis  
Presented to  
The Academic Faculty

by

Qiyong Fan

In Partial Fulfillment  
of the Requirements for the Degree  
Master of Science in Medical Physics in the  
School of Mechanical Engineering

Georgia Institute of Technology  
December 2010

# EMISSION GUIDED RADIATION THERAPY: A FEASIBILITY STUDY

Approved by:

Dr. Lei Zhu, Advisor  
School of Mechanical Engineering  
*Georgia Institute of Technology*

Dr. Sang Hyun Cho  
School of Mechanical Engineering  
*Georgia Institute of Technology*

Dr. C.-K. Chris Wang  
School of Mechanical Engineering  
*Georgia Institute of Technology*

Date Approved: September 29, 2010

## ACKNOWLEDGEMENTS

First of all, I would like to thank my advisor Dr. Lei Zhu, without whom this work could not have been possible, for his persistent and invaluable guidance on this work. It has been a great pleasure and a privilege to study and do research under his supervision. Dr. Zhu not only possesses the incredible foresight on my work but also is always able to guide me through the technical difficulties. Moreover, I would like to thank my thesis committee, Dr. Sang Hyun Cho and Dr. C.-K. Chris Wang for their helpful comments and suggestions to make this thesis better in various aspects. Also, thanks for their useful suggestions on the future work of this study. Finally, I would like to thank Dr. Paul Segars from Duke University School of Medicine to provide us with the XCAT phantom, Dr. Samuel Mazin and Mr. Akshay Nanduri from Stanford University School of Medicine and Reflexion Medical Inc. for useful information and discussions, Dr. Youngho Seo from University of California at San Francisco for his help in data reference, and Dr. Tianye Niu from our group for help in implementing the algorithms.

# TABLE OF CONTENTS

<b>ACKNOWLEDGEMENTS</b> . . . . .	<b>iii</b>
<b>LIST OF FIGURES</b> . . . . .	<b>vi</b>
<b>SUMMARY</b> . . . . .	<b>ix</b>
<b>I BACKGROUND AND INTRODUCTION</b> . . . . .	<b>1</b>
1.1 Overview of radiation therapy . . . . .	1
1.2 Treatment margins . . . . .	2
1.3 Difficulties of current radiation therapy practice . . . . .	4
1.4 Other approaches and emission guidance as a viable choice . . . . .	6
1.5 Our proposed approach . . . . .	7
<b>II SIMULATION TOOLS</b> . . . . .	<b>9</b>
2.1 Overview . . . . .	9
2.2 Simulation packages . . . . .	10
2.2.1 MOSEK . . . . .	10
2.2.2 GATE . . . . .	10
2.2.3 VMC++ . . . . .	11
2.3 Treatment planning . . . . .	14
<b>III EGRT IN IMRT</b> . . . . .	<b>16</b>
3.1 Overview . . . . .	16
3.2 Proposed EGRT IMRT system design . . . . .	17
3.3 PET detector arrangement . . . . .	17
3.4 Tumor localization . . . . .	19
3.5 Treatment plan modification . . . . .	21
3.6 Treatment scheme in IMRT . . . . .	23
3.7 Evaluation . . . . .	24
3.7.1 Overview . . . . .	24
3.7.2 Reconstruction and localization . . . . .	26

3.7.3	Two simulation cases . . . . .	27
3.8	Results . . . . .	29
3.8.1	Pancreas tumor case . . . . .	29
3.8.2	Lung tumor case . . . . .	32
<b>IV</b>	<b>EGRT IN TOMOTHERAPY . . . . .</b>	<b>35</b>
4.1	Overview . . . . .	35
4.2	Proposed EGRT tomotherapy system design . . . . .	35
4.3	Planning sinogram, emission sinogram and treatment plan modification	36
4.4	Adaptive dose delivery . . . . .	38
4.5	Treatment scheme in tomotherapy . . . . .	40
4.6	Evaluation . . . . .	40
4.6.1	Overview . . . . .	40
4.6.2	Geometry of evaluation phantom . . . . .	41
4.6.3	Optimization . . . . .	43
4.6.4	Concept of treatment without margins . . . . .	44
4.7	Results . . . . .	45
<b>V</b>	<b>DISCUSSION, CONCLUSION AND FUTURE WORK . . . . .</b>	<b>47</b>
5.1	Discussion and conclusion . . . . .	47
5.2	Future work . . . . .	49
	<b>REFERENCES . . . . .</b>	<b>51</b>

## LIST OF FIGURES

1	Illustration of tumor volumes including GTV, CTV and PTV that lead to margin concept. OAR is organ at risk and ITV refers to internal target volume. . . . .	3
2	A typical IGRT process including mainly three steps. . . . .	4
3	Illustration of GATE simulation system. The whole system is defined in a cubic volume called <b>world</b> . Calculation is done only for particles in world volume. The ring detector system is placed around the isocenter of the world volume. The voxelized phantom can be read in to be put in the isocenter of the volume. . . . .	12
4	Illustration of VMC++ geometry(1). Here defines the geometry of one simulation example. Sources are placed in different positions. The cross section of radiation is defined by beamlets. . . . .	13
5	Illustration of VMC++ geometry(2). Here shows the dose output images of the phantom after the radiation is delivered. . . . .	14
6	The schematic diagram of the proposed EGRT system for IMRT scheme. Left: the tumor tracking using radioactive tracers; Right: Dose delivery with the help of detected tumor motion position for one particular field. . . . .	17
7	The proposed EGRT system design of two investigated PET detectors arrangements. The EGRT system is a hybrid system, consisting of a Linac and PET detectors. Left: shows the PET detectors arrangements with OBI devices, Right: shows the PET detectors arrangements without OBI devices. . . . .	18
8	Illustration of localization method. . . . .	20
9	2D illustration of treatment plan modification method. . . . .	22
10	A summary of EGRT treatment scheme. The treatment scheme is composed of two parts: tumor localization and dose delivery. The updated tumor location obtained by reconstruction and localization algorithms will be used to modify the treatment plan to finally achieve a successful treatment. . . . .	24
11	A chart flow of method evaluation. The method evaluation is also divided into two parts similarly and used to simulate the whole process of treatment scheme of EGRT. . . . .	25
12	The XCAT phantom images of pancreas tumor case and its reconstructed tumor images. . . . .	28

13	The XCAT phantom images of pancreas lung case and its reconstructed tumor images. . . . .	29
14	The reconstructed images of pancreas tumor case with specific angle coverage of 240°, 180° and 120°. . . . .	30
15	The locating accuracy of different detector angle coverage for both arrangements. . . . .	31
16	The dose distribution and DVH for pancreas tumor case if setup error exists without EGRT. The tumor is in red color; other colored organs are the organs at risk. . . . .	31
17	The dose distribution and DVH for pancreas tumor case if setup error exists with EGRT. The tumor is in red color; other colored organs are the organs at risk. . . . .	32
18	Fluence map modification. Upper: before modification; lower: after modification. The numbers indicate the field angles. . . . .	32
19	The locating accuracy of lung tumor case for full detector coverage. . . . .	33
20	The locating accuracy of lung tumor case for 150 degree coverage. . . . .	33
21	The dose distribution and DVH for lung tumor case if setup error exists with EGRT based on gating delivering technique. The tumor is yellow color; other colored organs are the organs at risk. . . . .	33
22	The schematic diagram of the proposed EGRT system for tomotherapy scheme. . . . .	36
23	Sinograms involved in simulations to demonstrate concept of treatment without using margins. Emission sinogram will be shifted if setup error exists, then we can modify the planning sinogram according to the shift amount of Emission sinogram. . . . .	38
24	Adaptive dose delivery of EGRT tomotherapy. . . . .	39
25	Compensation method in adaptive dose delivery. . . . .	40
26	Treatment scheme of EGRT tomotherapy. . . . .	41
27	Method of Evaluation for EGRT Tomotherapy. . . . .	42
28	Geometry involved in simulations. . . . .	43

29	Dose distribution of treatment without using margins. The number on isodose line is the percentage of prescribed dose. Geometry is the same as Figure 28(b). Left: dose distribution without any method if setup error exists, corresponding to Figure 30(a). Right: dose distribution using proposed method even if setup error exists, corresponding to Figure 30(b). . . . .	45
30	DVHs of treatment without using margins. . . . .	46



## SUMMARY

Accurate tumor tracking remains as a major challenge in radiation therapy. Large margins are added to the clinical target volume (CTV) to ensure the treatment of tumor in presence of patient setup uncertainty and that caused by intra-fractional motion. Fiducial seeds and calypso markers are commonly implanted into the disease sites to further reduce the dose delivery error due to tumor motion. For more accurate dose delivery and improved patient comfort, the use of radioactive tracers in positron emission tomography (PET) as non-invasive tumor markers has been proposed - a concept called emission guided radiation therapy (EGRT). Instead of using images obtained from a stand-alone PET scanner for treatment guidance, we mount a positron imaging system on a radiation therapy machine. Such an EGRT system is able to track the tumor in real time based on the lines of response (LOR) of the tumor positron events, and perform radiation therapy simultaneously. In this work, we propose a typical treatment scheme for EGRT and validate the EGRT concept using computer simulations. EGRT can be implemented in any modality where tumor tracking is needed, such as Intensity-Modulated Radiation Therapy (IMRT) and tomotherapy. EGRT's advantage on increased dose delivery accuracy is demonstrated using a pancreas tumor case and a lung tumor case without the setup margin and motion margin for IMRT treatment and using a prostate tumor case without setup margin for tomotherapy treatment. The emission process is simulated by Geant4 Application for Tomographic Emission package and Linac dose delivery is simulated using a voxel-based Monte Carlo algorithm. The tumor tracking error can be controlled within about 3 mm which indicates margins can be significantly reduced. The dose distributions show that the proposed EGRT can accurately deliver the prescribed

dose to the CTV with much smaller margins. Although still in a preliminary research stage, EGRT has the potential to substantially reduce tumor location uncertainties and to greatly increase the performance of current radiation therapy.

# CHAPTER I

## BACKGROUND AND INTRODUCTION

### *1.1 Overview of radiation therapy*

Radiation is intensively involved in the two most important research topics in medical physics, which are medical imaging and radiation therapy. In medical imaging, radiation is used for cancer diagnosis; while in radiation therapy, radiation is used to control and destroy malignant cells in order to perform cancer treatment. Although imaging and therapy are quoted as two separate research sub-fields, imaging is actually involved in every key step of therapy such as computed tomography (CT) simulation, treatment planning and radiation delivery.

Since radiation therapy was first used, its development is tightly connected with the evolution of imaging techniques[23]. In other words, radiation therapy is essentially imaging-orientated and imaging-guided. In early days when x-ray was first discovered, radiologists located the tumor by making use of 2-dimensional (2D) transmission images of human body. Later on due to the emergence of CT, the tumor is targeted with highly conformal dose distribution with the help of 3-dimensional (3D) reconstructed CT images. This huge improvement from 2D to 3D resulted in significant dose reduction to normal tissues and more uniform dose distribution inside the tumor volume, which dramatically increase the tumor control probability. Recent technical advances brought up the intensity-modulated radiation therapy (IMRT) which has further enhanced this improvement[5][6].

However in practice, unpredictable uncertainties exist in multiple processes such as tumor volume delineation or target localization due to reasons such as intra- and inter-organ motion. Without reducing these uncertainties, IMRT technique will not

be able to fully exhibit its advantages on cancer treatment. Therefore, intensive research activities recently focus on image-guided radiation therapy (IGRT) to eliminate such uncertainties, especially that in tumor tracking in order to strengthen the power of IMRT techniques. Here IGRT mainly refers to the new technologies employed in the processes of radiation planning, patient setup and in the procedures of delivery, in which cutting-edge image-based tumor definition methods, patient positioning devices, motion management tools and radiation delivery guiding tools are used[23]. The ultimate goal of IGRT is to locate the tumor with high accuracy and to verify this accuracy in the radiation delivery process in order to ensure the tumor is treated as planned.

Clinically, two types of therapy scheme are typically available: external beam therapy and tomotherapy. Different from external beam therapy, in tomotherapy, radiation is delivered slice by slice with image guidance. Therefore, IGRT can be and is actually applied in both therapy schemes.

## ***1.2 Treatment margins***

A radiation treatment margin is routinely used in radiation therapy and is very important for clinical radiotherapy[4]. It mainly refers to the area of healthy tissue around the target area that also receives radiation. The radiation treatment margin may be the tissue around an existing tumor, or around a lumpectomy cavity. Part of the goal of the radiation therapy is to find out ways to reduce treatment margins as much as possible, so that less healthy tissue is affected by radiation.

The concept of gross tumor volume (GTV), clinical target volume (CTV) and planning target volume (PTV) is essential to understand the margin concept. GTV is the gross demonstrable extent and location of the tumor, which may consist of primary tumor, metastatic lymphadenopathy, and other metastasis. The GTV is usually based on information obtained from a combination of imaging modalities (CT,

MRI, ultrasound, etc.), diagnostic modalities (pathology and histological reports, etc.) and clinical examination. CTV consists of demonstrated tumor(s) if present and any other tissue with presumed tumor, representing true extent and location of tumor. This volume has to be treated adequately in order to achieve the aim of therapy, cure or palliation. PTV consists of CTV plus an internal margin (margin for internal physiological movements) plus an additional margin for patient movement and set-up uncertainty. Margin has to be large enough to compensate for both internal movements and set-up uncertainty. The illustration of these tumor volumes and margins is shown in Figure 1.

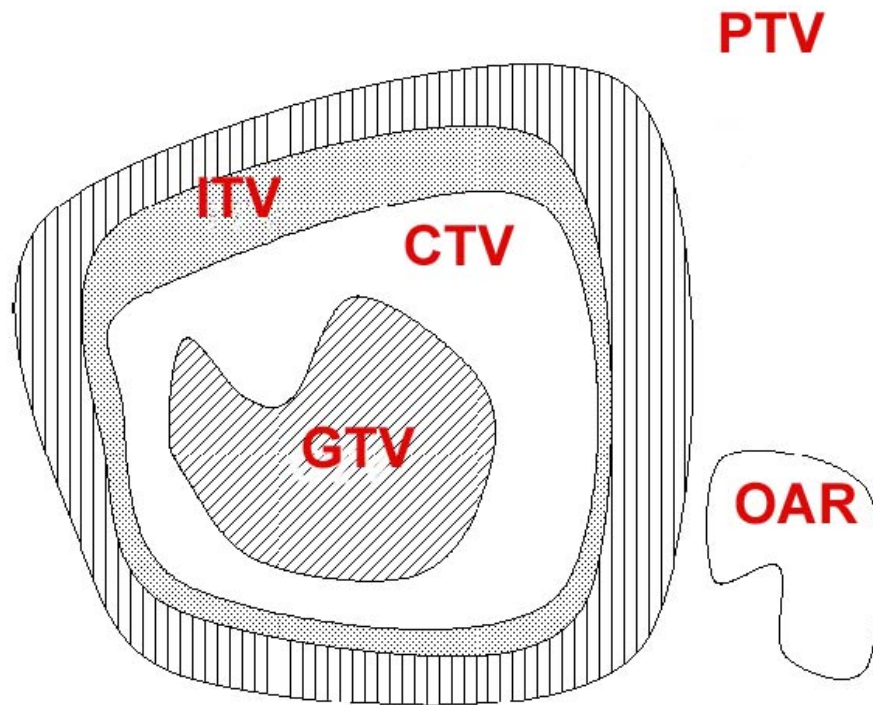


**Figure 1:** Illustration of Tumor volumes including GTV, CTV and PTV that lead to margin concept. OAR is organ at risk and ITV refers to internal target volume.

Usually margins depend on organ motion which causes internal margins, and patient set-up and beam alignment which brings external margins. The internal margin is designed to take into account the variations in the size and position of the

CTV relative to the patient’s reference frame (usually defined by the bony anatomy), i.e., variations due to organ motions such as breathing, bladder or rectal contents, etc. The external margins are mainly caused by setup uncertainties, machine tolerances and intra-treatment variations. Margins can be non-uniform but should be three dimensional. A thumb of rule of determining magnitude of margins is that the target is in the treated field at least 95% of the time. In this work, the internal margins are mainly represented by motion margins (margins caused by motion) while the external margins are mainly represented by setup margin (margins caused by setup error). One goal of this study is to reduce margins so as to achieve treatment with few or even no margins, including motion margins and setup margins by our proposed accurate tumor tracking method.

### 1.3 Difficulties of current radiation therapy practice

In current radiation therapy practice, IGRT is widely used clinically. As for dose delivery tool, Varian’s medical system has broad applications. For example, Varian Trilogy Linac, Varian HDR Brachytherapy system and so on. One typical IGRT process based on Varian’s Linac system is shown in Figure 2.

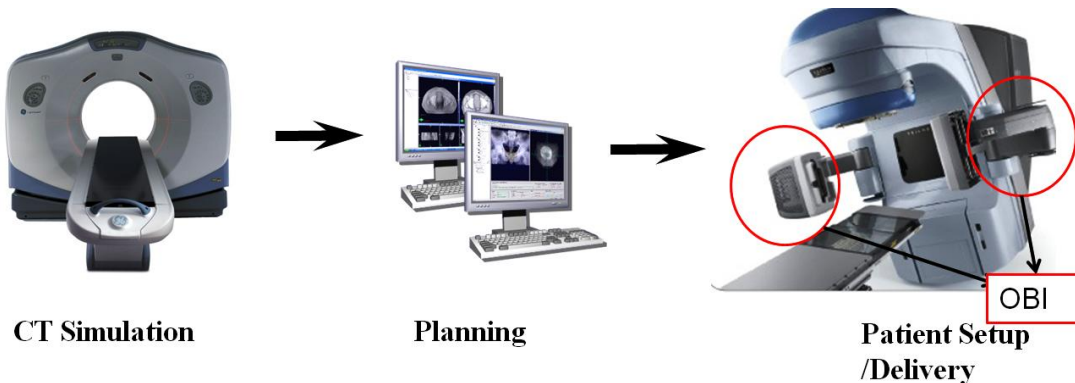


**Figure 2:** A typical IGRT process including mainly three steps.

One such typical IGRT process starts from CT simulation where patient anatomy CT images are acquired. Based on the fusion images of MRI and CT images, the

treatment plan can be generated to treat the tumor in the planned position. The planned position is defined as the tumor position in the CT/MRI fusion images contoured by the responsible physicians or residents. Thereafter, the patient is setup by the radiotherapist with the help of various immobilization tools such as thermal masks and wing board, whose purpose is to ensure that the patient is set up in the planned position. The on board imager (OBI) is used further to adjust the patient position with the help of bone anatomy landmarks and verify that the tumor is in the planned position, manually by radiotherapist. However, this method adjusts the position in an indirect way, which decreases its effectiveness.

For the process stated above, although IGRT may significantly improve the radiation therapy performance, it still currently encounters remarkable difficulties in locating the tumor precisely, especially for the tumor in motion. One of the biggest difficulties comes from the fact that the tumor locating method is an indirect one which makes it essentially imprecise. For example, the immobilization devices fix the patient to ensure that the patient is always in the same position for every fractionated treatment. However, setup error still exists in spite of those immobilization devices which means even if the fixed position can be made always the same for every treatment it may not be exactly the same as planned. Another example is the OBI. OBI is used as image guidance to further verify the patient is in the appropriate position. However, OBI aligns the patient according to the bony anatomy structures rather than the real tumor tissues. This will inevitably bring errors, especially those from therapist operations.

Another essential difficulty comes from the motion which includes the organ motion, tumor motion, and patient motion. Current radiation therapy practice could not actually deal with the small irregular motion caused by organ motion and patient motion which may exist in a significant amount of cancer types. For large periodic motion like respiratory movement, although gating technique has been proposed[16],

this method is not accurate because the respiratory motion only has a rough pattern and cannot be accurately determined using gating technique itself. Besides, this method assumes that the tumor motion is consistent or has the same pattern with the marker motion, which is very likely not the case and still in debate. Therefore, fiducial markers or Calypso are commonly used[3][10]. However, they are invasive, which causes significant patient discomfort, and thus cannot achieve a satisfactory performance.

Due to all the issues discussed above, IGRT still cannot achieve its ultimate goal of locating the tumor with sufficiently high accuracy in an optimal way. Therefore, large margins, typical in magnitude of several centimeters, are added to CTV and even more for GTV[13][20]. To further improve the tumor tracking accuracy and reduce the tumor margins, other solutions are needed. The new solution needs to either address those difficulties of IGRT or bring new techniques that are free of those disadvantages.

#### ***1.4 Other approaches and emission guidance as a viable choice***

Setup error can be viewed as one-time motion. Therefore, the dilemma of current IGRT practice is essentially motion problem. Several attempts to solve tumor motion problem have already been discussed briefly in previous sections. Here this topic is examined further in the following. These attempts are either actually commercially available or under development, which include X-ray guided therapy[12], respiratory gating[14], implantable beacons and MRI guided therapy[18]. However, X-ray imaging is not a good choice since it only has poor soft-tissue contrast. Most existing systems rely on tracking fiducial markers or bony anatomy to determine or predict tumor location. Respiratory gating is ineffective and inaccurate, since it assumes the motion of the marker is consistent with the lung motion, which is still in debate. In addition, the human breathing cycle is variable in nature. Fiducials or beacons are



not suitable for all patients with lung tumor since the use of them may introduce lung collapse[1]. Moreover, implantable markers can also drift during treatment. Low-field MRI generally is not able to generate good quality volumetric images[17], while high-field MRI will introduce dose **hot-spots** outside of the target volume because of the electron return effect.

In search of an alternative method for real-time tumor tracking which is the main dilemma of current IMRT and IGRT practice, emission guidance becomes a viable approach. Emission guidance refers to the guidance provided by any radioactive tracer emission originating from the tumor site. In this work, positron emission is mainly studied. Positron emission (PE) is mainly studied since line of response (LOR) of PE naturally defines the projection line to localize the tumor. Currently the most common application of positron emission is Positron Emission Tomography (PET). PET is emerging as the imaging standard in cancer diagnosis, offering higher sensitivity and specificity compared to all other imaging modalities across the majority of cancer types[19]. With the use of a radio-labeled tracer such as  $^{18}\text{F} - \text{FDG}$ , PET depicts metabolic activity, and makes tumors to **light up**. Other PET tracers such as F-MISO and FLT can show other characteristics of tumors such as hypoxia and proliferation. Despite these distinct advantages, PET has not been incorporated into real-time adaptive radiation therapy since it takes minutes to generate a full image. That is, PET or PE is not currently used during treatment. However, we may not need a full PET image to locate the tumor, so it is possible to include PET or rather positron emission into real-time adaptive radiation therapy. This is where we start to propose a new approach and its corresponding system to guide radiation therapy.

### ***1.5 Our proposed approach***

In order to address the issues of IGRT and based on the discussion in last section, we propose a novel and practicable approach to directly guide radiation therapy, a

concept called Emission Guided Radiation Therapy (EGRT). The work presented in this thesis will mainly introduce the concept, the EGRT system design and then validate the concept through simulation study for two therapy schemes which are IMRT therapy scheme and tomotherapy therapy scheme.

The EGRT concept is straightforward. Emission guidance refers mainly to the guidance provided by the emission events of the radioactive tracers, for example  $^{18}F-FDG$ , which is injected into patient before radiation delivery. After injection, the radioactive tracers will concentrate in the tumor due to highly active metabolism and thus positron emission will occur mainly in the disease sites, highlighting the tumor site. When emission guidance is incorporated into simultaneous radiation delivery, tumor lights up and can be located directly in almost real time which will solve the dilemma of IGRT discussed before. For hardware to achieve this, we mount PET detectors onto a typical Linac system, arranged symmetrically around the isocenter of the system gantry.

The advantages of EGRT are obvious and various. First of all, EGRT is noninvasive because the radioactive tracers are noninvasive and can be injected into patient easily based on current nuclear medicine technique. Also, in EGRT, the functional information is presented which is good for therapy purpose. Moreover, EGRT is a direct method of locating tumor in almost real time, quite different from the indirect tumor tracking method such as IGRT. Besides, through our simulation, EGRT shows high accuracy of tumor tracking. In this case, very small margins or even no margins are needed due to the fact the tumor can be located almost in real time and there is no need to use large margins to compensate for those certainties discussed. This is why the concept of treatment without margins is possible.

## CHAPTER II

### SIMULATION TOOLS

#### *2.1 Overview*

Simulation is a good way to validate the proposed EGRT concept since the concept can be tested easily and effectively without building a real system. However, practical simulations should be carried out to make the simulations convincing. Thus, effective simulation tools are needed. As for the validation of EGRT concept, two sets of simulation tools are needed. One is needed to simulate the process of tumor localization, i.e. whether the tumor can be located in almost real time and how accurate it would be, and the other one is needed to simulate the process of dose delivery according to the dynamically determined tumor position. In the tumor localization part, Geant4 Application for Tomographic Emission (GATE) package, a GEANT4 based dedicated Monte Carlo simulation tool for positron emission, is used to simulate the process of positron emission after the radioactive tracers are injected into the patient. The data output of GATE is then used to determine the position of the tumor; while in the dose delivery part, voxel base Monte Carlo package VMC++ and optimization package MOSEK is used to determine the dose kernel for making treatment plan and computing dose distribution and beamlet intensity. For both parts, realistic human phantom is needed to do such evaluation and XCAT phantom is applied for this purpose. Besides the simulation tools, the treatment planning will also be discussed in this chapter because it is a common method for both therapy schemes which will be discussed in the following two chapters.

## ***2.2 Simulation packages***

### **2.2.1 MOSEK**

MOSEK is an optimization package for making treatment plan in this work. The MOSEK optimization package can be used to solve large-scale mathematical optimization problems[2]. MOSEK provides fast and efficient specialized solvers for a lot of types of optimization problems including linear problems, quadratic problems, general convex problems and mixed integer problems. This package can be used with various interfaces including C/C++, .NET, Java and Python. In this work, MOSEK MATLAB optimization tool box is called to run MOSEK optimization codes. The optimization problem of treatment planning is illustrated in the treatment planning section.

### **2.2.2 GATE**

GATE, short for Geant4 Application for Tomographic Emission, is a PET/SPECT dedicated simulation platform based on Geant4, an opensource package developed by the international OpenGATE collaboration[21]. GATE can be run on multiple operating system platforms including Window and Linux. In this work, GATE is run in Ubuntu 8.10. GATE is dedicated to the numerical simulations in medical imaging, especially for simulations of Emission Tomography (Positron Emission Tomography - PET and Single Photon Emission Computed Tomography - SPECT). Due to the fact that GATE coding can be done using an easy-to-learn macro mechanism and highly sophisticated experimental settings can be easily configured, GATE now plays a key role in the design of new medical imaging devices, in the optimization of acquisition protocols and in the development and assessment of image reconstruction algorithms and correction techniques[21].

In order to understand how GATE works, a summary of steps to write a GATE script is given below:

1. Define the scanner geometry
2. Define the phantom geometry
3. Set up the physics process
4. Initialize the simulation
5. Set up the detector model (digitizer)
6. Define the sources
7. Specify the data output format
8. Start the data acquisition

GATE is not only able to construct user-defined phantom, but also able to read in voxelized phantom. A picture of GATE simulation is shown in Figure 3.

One of the data outputs of the GATE simulation is the coincidence counts information which records where the coincidence events are detected. In this work, this is the main data output to be used.

### **2.2.3 VMC++**

VMC++ is a highly efficient Monte Carlo dose calculation engine for radiation therapy treatment planning[9][8]. It has been validated against well established codes. VMC++ can be easily installed and run under any PC that uses a DOS shell. The main command of running VMC++ is shown below:

```
vmc.exe    input_file
```

Therefore, in order to run the VMC++ for the wanted simulation, the main task is to write an input file which includes the following information:

- The geometry of the simulated phantom

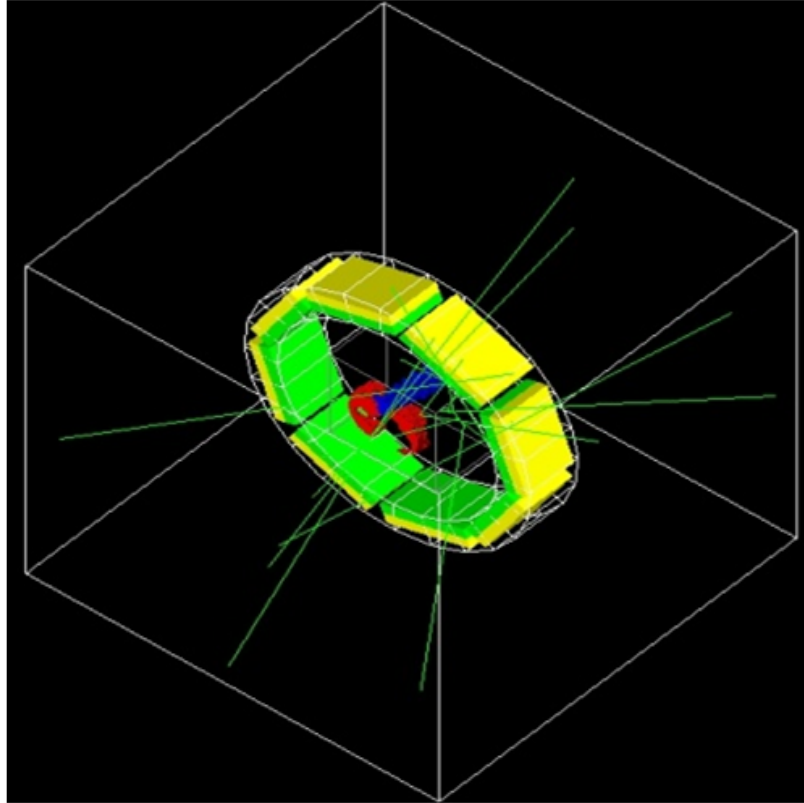


**Figure 3:** Illustration of GATE simulation system. The whole system is defined in a cubic volume called **world**. Calculation is done only for particles in world volume. The ring detector system is placed around the isocenter of the world volume. The voxelized phantom can be read in to be put in the isocenter of the volume.

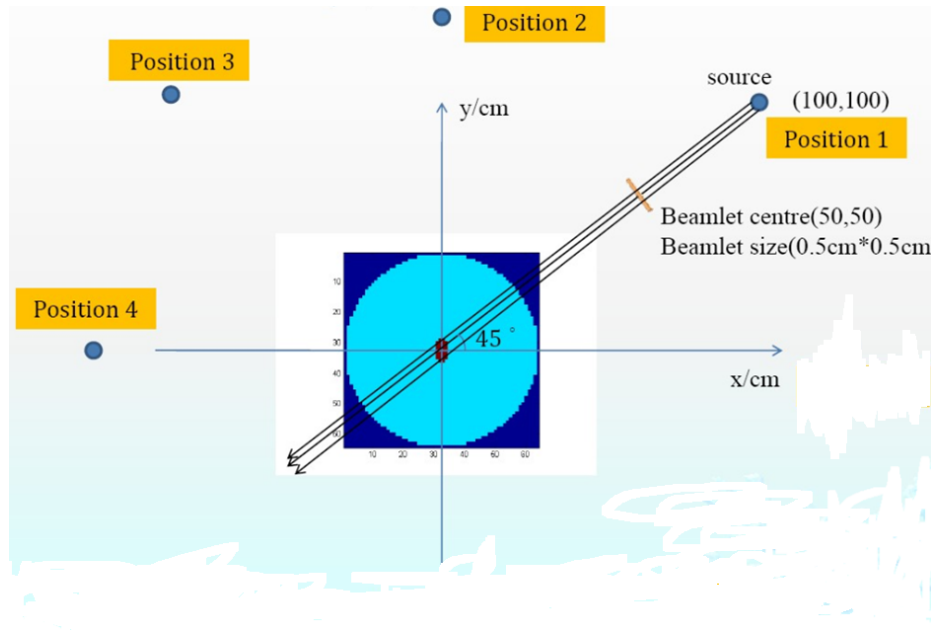


**Figure 4:** Illustration of VMC++ geometry(1). Here defines the geometry of one simulation example. Sources are placed in different positions. The cross section of radiation is defined by beamlets.

- Defined source position and beamlet edges coordinates
- Source spectrum
- Defined Monte Carlo simulation parameters

One input file only includes one point source and one beamlet. The beamlet is usually placed in the midpoint between the point source and geometry isocenter. Therefore, one simulation will need hundreds or even thousands of input files, depending on how many beams are needed. For each input file, it will generate a line of radiation and the beamlet edges coordinates need to be defined to give the cross section of this line of radiation because only the dose from the radiation that goes through the beamlet will be calculated. Thus the cross section of this line of radiation can be tuned by changing the beamlet edges parameters. One illustration of VMC++ is shown in Figure 4 which defines the geometry of one simulation example and in Figure 5 which gives the corresponding dose output.

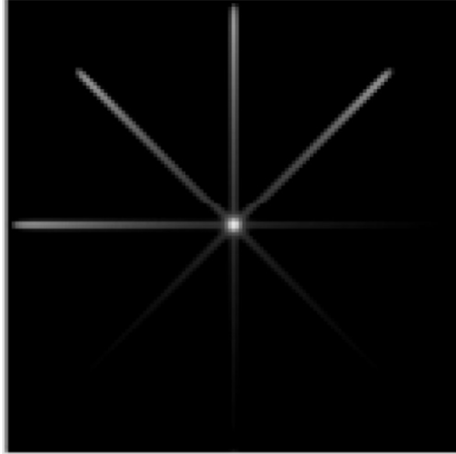


**Figure 5:** Illustration of VMC++ geometry(2). Here shows the dose output images of the phantom after the radiation is delivered.

Based on the characteristics of VMC++, it is used in this work as the simulation tool for getting the dose distribution of the radiation delivered by a typical Linac in the phantom. Each output for each input file of the VMC++ is a 3D dose distribution for the specified point source defined in the input file that penetrates the phantom, also called the dose kernel.

### ***2.3 Treatment planning***

For treatment plan, inverse treatment planning technique is typically used in current radiation therapy. It is usually used to optimize the treatment beam apertures and weights such that the delivered dose on the patient is as close as possible to the prescribed dose[24]. The delivered dose distribution on the patient,  $d$ , has a linear relationship with the intensity of the beamlets,  $x$

$$d = Ax$$

where  $d$  is the vectorized 3D dose distribution and the beamlet intensity  $x$  is a 1D vector that consists of rowwise concatenations of beamlet intensities for all fields[24]. Each column of matrix  $A$  is a beamlet kernel, corresponding to the dose distribution achieved by one beamlet with unit intensity for all the considered voxels.



Typically the sum of the square errors of the delivered dose relative to the prescribed dose is used as the optimization objective function. Therefore, the treatment planning problem can be expressed as

$$\begin{aligned} & \text{minimize} \\ & \sum_i \lambda_i (A_i x - d_i)^T (A_i x - d_i) \\ & \text{subject to} \\ & x \geq 0 \end{aligned}$$

where the index  $i$  denotes different structures;  $\lambda_i$  is the relative importance factor[15][22]; each column of matrix  $A_i$  is the beamlet kernel corresponding to the  $i$ th structure, and  $d_i$  is the prescribed dose for the  $i$ th structure. The same form of objective functions for both the target and the critical structures is used, however, a low prescribed dose is used for the critical structures. Through the use of optimization package, all the beamlet intensities can be obtained and thus a treatment plan can be made.

## CHAPTER III

### EGRT IN IMRT

#### *3.1 Overview*

EGRT is a concept of guidance in radiation therapy. Therefore, EGRT can be applied in different modalities where tumor tracking is needed, e.g. IMRT and tomotherapy. In IMRT treatment, the position will first be determined to reduce the setup uncertainties and then monitored in almost real time to aid the radiation delivery process. In tomotherapy treatment, the situation is slightly different. The tumor position is gradually determined with an adaptive dose delivery scheme. In this work, both IMRT scheme and tomotherapy scheme are investigated. This chapter will discuss the case of IMRT scheme.

In both treatment schemes, we have used the concept of sinogram. The sinogram concept in this work is similar to that in CT reconstruction. There are two parameters associated with this concept, which is the angle of the LOR relative to the isocenter of the whole system, and the displacement of LOR relative to the isocenter respectively. The intensity of the sinogram is the number of counts or LORs that have the same angle and displacement. In current simulation the two parameters are sampled and thus discrete. The sample period is optimized according to phantom voxel size and reconstruction resolution.

There are two key issues needed to be addressed in EGRT concept. One is tumor tracking, question may include how to locate the tumor in real time and what is the locating accuracy; the other is treatment plan modification algorithm, question may include how to effectively modify treatment plan based on tumor position and does the modified plan work for treatment. These two issues are important in both IMRT

scheme and tomotherapy scheme. The main content in this chapter will focus on how to address those questions for IMRT scheme and the main content in next chapter will focus on how to answer those questions for tomotherapy scheme.

### 3.2 Proposed EGRT IMRT system design

In EGRT IMRT scheme, Linac delivers the dose in a similar way as it does in current radiation therapy practice by using the tumor location information obtained by the PET detectors. A schematic diagram of EGRT system for IMRT scheme is shown in Figure 6. Such a system is able to determine the tumor location by using PET

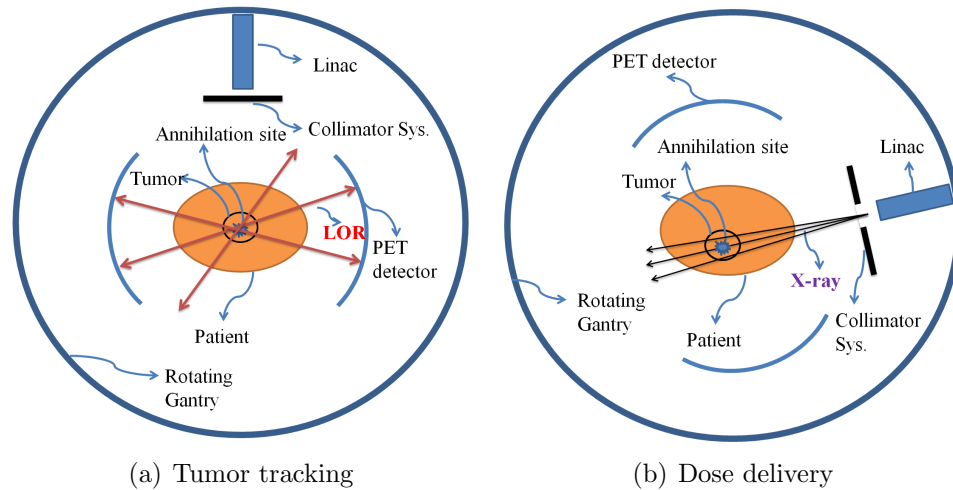


**Figure 6:** The schematic diagram of the proposed EGRT system for IMRT scheme. Left: the tumor tracking using radioactive tracers; Right: Dose delivery with the help of detected tumor motion position for one particular field.

detectors and also to deliver the dose instantly through a treatment plan modification process based on the tumor location information. In this case, positron imaging is integrated into treatment used as guidance.

### 3.3 PET detector arrangement

The purpose and feature of EGRT system is to deliver the radiation while tracking the tumor in real time and then improve the treatment performance based on the dynamically acquired tumor location. Therefore, the EGRT system is designed to be

a hybrid system, consisting mainly of a Linac accelerator and PET detectors. They are arranged such that the tumor position could be detected, monitored and used to aid the process of dose delivery simultaneously. Unlike as used in PET imaging where detection is the main purpose, PET detectors cannot occupy the whole ring because of the existence of the Linac and possible OBI devices. Thus, it is very important to find out whether the tumor can be located in such EGRT system where only limited PET detector coverage is available and further how much PET coverage is needed to get a reasonable locating accuracy. In order to take this realistic situation and consideration into account, two schemes of PET detector arrangements, which is system with OBI arrangement and system without OBI arrangement, have been investigated, shown in Figure 7(a) and (b).

For arrangement (a), four pieces of PET detectors are centered around the isocenter and the angle  $\theta_1$  is defined as the angle coverage of a single PET detector and is symmetrical about the  $45^\circ$  axis, while in arrangement (b), two pieces of PET detectors are also centered around the isocenter however the angle  $\theta_2$  is defined as the angle coverage of one PET detector and is symmetrical about the  $x$  axis.

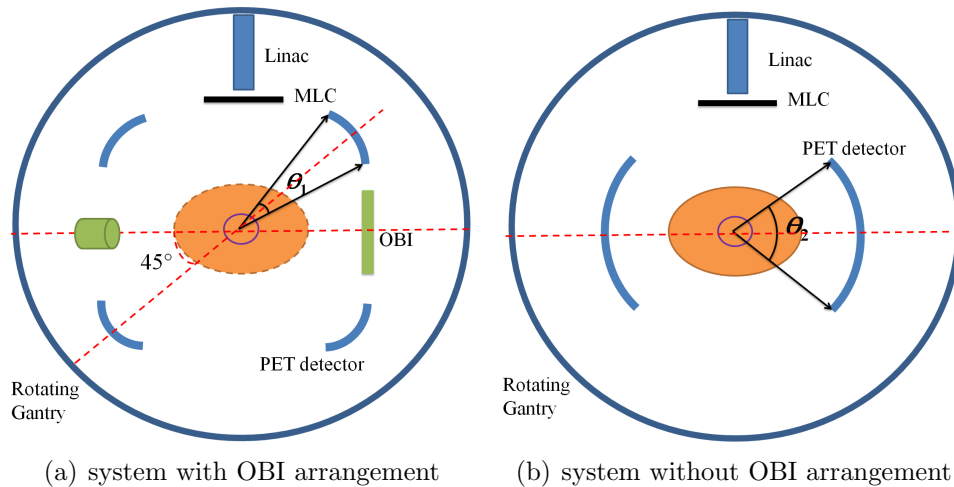


**Figure 7:** The proposed EGRT system design of two investigated PET detectors arrangements. The EGRT system is a hybrid system, consisting of a Linac and PET detectors. Left: shows the PET detectors arrangements with OBI devices, Right: shows the PET detectors arrangements without OBI devices.

Obviously, for arrangement (a), the total detector coverage is equal to  $4\theta_1$  while for arrangement (b), the total detector coverage is equal to  $2\theta_1$ . For the same detector coverage, it is expected that the system with OBI arrangement be able to detect the tumor position more accurately because the collected data is more uniformly distributed in all directions.

Several issues and challenges need to be handled for such an EGRT system. One of them is to localize the tumor using incomplete LORs data since some LORs escape because of the partial detector coverage. A second challenge comes from the background signals when background tissue has an uptake ratio that is close to or even higher than that of the tumor. The reasonable uptake ratio should be determined that achieves acceptable EGRT performance. Another challenge is how fast the EGRT system may track the tumor location. Without a good time resolution, EGRT system may not exhibit its power on tumor tracking, especially for lung tumor motion.

### ***3.4 Tumor localization***

The tumor localization method described in this work is one way to make use of emission guidance for IMRT treatments, designed to be efficient and practical. The purpose of the tumor localization is to determine the real-time tumor location and further use it to achieve a satisfied treatment with acceptable dosimetry performance. Once the tumor position is determined to be different as the planned one, treatment plan needs to be modified instantly to take this position shift into account in order to still achieve the planned dose distribution. After the radioactive tracer injection, GTV will start to emit positrons and thus LORs can be determined based on the coincidence events. These LORs data are first reorganized into sinogram and the sinogram is then used to reconstruct the patient tumor image with background present. In the reconstructed images, since the tumor usually has higher uptake of radioactive tracer,

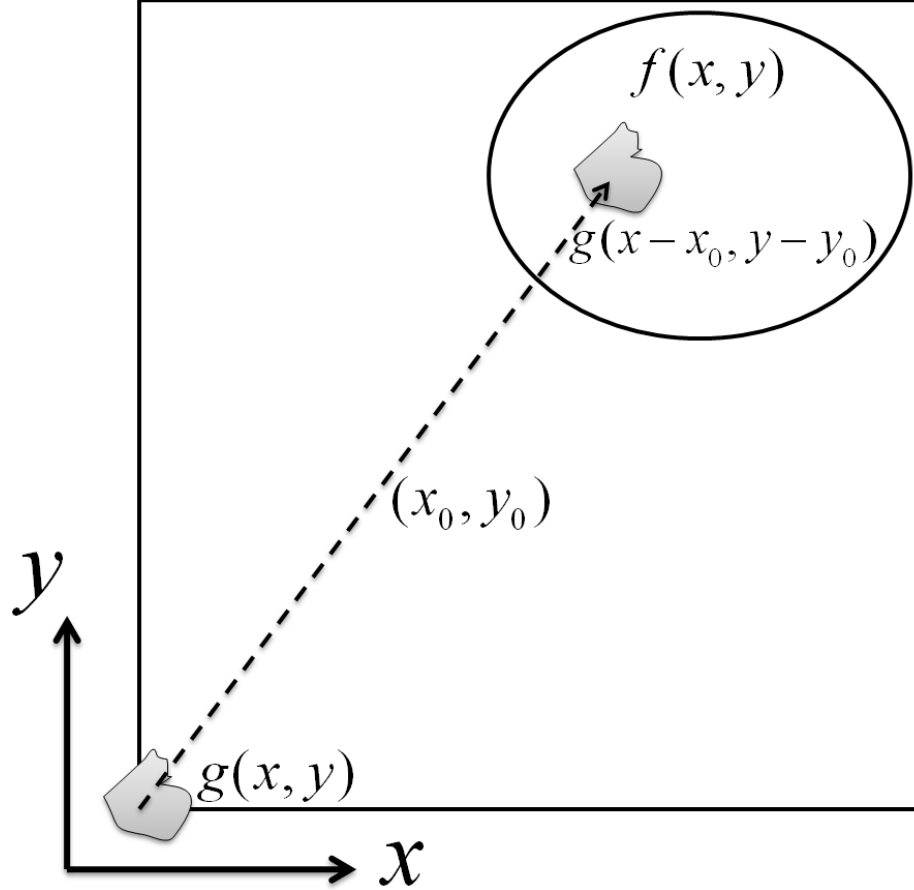


**Figure 8:** Illustration of localization method in 2D case.

it will have higher reconstructed image values. Based on this difference between the tumor and background, the tumor contour, obtained from the CT simulation, can be then applied onto the reconstructed tumor images to find out tumor location which is determined to be the position that maximizes the sum of image values that fall into the tumor contour, assuming the tumor does not deform. Figure 8 gives an illustration of our localization method in 2 dimensional (2D) case.

The potential tumor region is represented by  $f(x, y)$  and the tumor contour by  $g(x, y)$ . Since we assume the tumor does not deform, the position of the tumor can be represented by one single point. Suppose initially the tumor contour is placed at origin of the reconstructed image space. The tumor contour is then moved into the potential tumor region by a vector  $(x_0, y_0)$ .  $(x_0, y_0)$  represents any point in potential

tumor region so that the tumor contour can be moved around the whole region by varying  $(x_0, y_0)$ . Based on the principle discussed above, the tumor position  $(x_*, y_*)$  is determined to be the point  $(x_0, y_0)$  that maximizes

$$\sum f(P)g(P)$$

for any point in tumor contour, where  $g(x, y)$  represents the tumor contour and is equal to 1,  $f(x, y)$  represents the reconstructed image values of the potential tumor region,  $P$  is any point in tumor contour. The computation of this process depends on the step size of tumor's moving around at both  $x$  and  $y$  directions, i.e. the interpolation intensiveness of the algorithm.

The localization accuracy can be affected by factors such as the number of events used to reconstruct the tumor images, the temporal resolution, locating algorithm effectiveness, data completeness and uptake ratio. Noise may degrade the reconstructed image quality and thus affect the locating accuracy. High temporal resolution may decrease the number of events for each phase and increase data noise. Interpolation intensiveness of the locating algorithm will have a significant influence on the accuracy. The incomplete LORs data will cause artifacts on reconstructed images and degrade localization accuracy. Low uptake ratio of tumor will make tumor more difficult to be identified. Therefore, in order to achieve the optimized localization accuracy, these factors need to be examined carefully.

### ***3.5 Treatment plan modification***

Typically the treatment plan keeps unchanged during the treatment since the tumor position change is taken into account by adding margins or using gating technique. However in EGRT, no margin is used and thus the treatment plan needs to be modified instantly as the tumor moves, allowing no time to be made anew and still achieving the planned tumor dose distribution with negligible errors.

The proposed treatment modification algorithm works as follows. The main idea

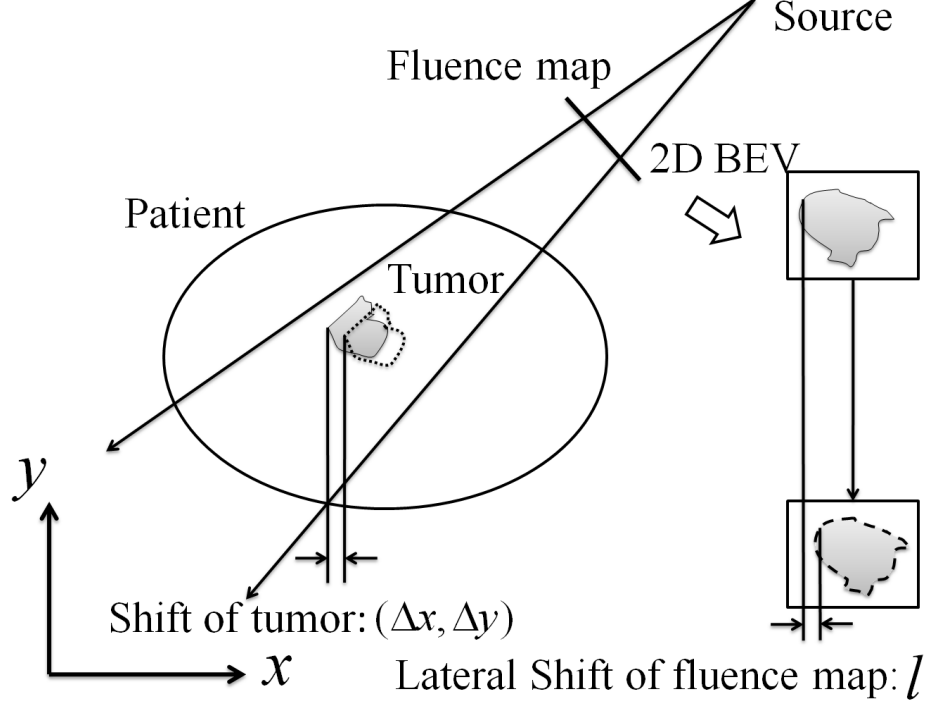


**Figure 9:** 2D illustration of treatment plan modification method.

is to shift the fluence map of each field to capture the tumor all the time. Figure 9 gives a straight illustration of this idea.

Suppose one IMRT treatment has  $N$  treatment fields, noted as  $\beta_i, i = 1, 2, 3, \dots, N$ . The tumor position change is noted as  $(\Delta x, \Delta y, \Delta z)$ . For all  $N$  fields, the fluence map is shifted in the plane of 2D beam eye's view (BEV) of each field with a magnitude calculated by the following formula:

$$l = \Delta x \cos(\beta_i) + \Delta y \sin(\beta_i), i = 1, 2, 3, \dots, N$$

$$a = \Delta z, i = 1, 2, 3, \dots, N$$

where  $l$  indicates the shift in lateral direction and  $a$  indicates the shift in axial direction. This shift can be done using a 2D cubic interpolation. After modification, the fluence map is ready to be used to deliver the dose to the tumor in shifted position. The dose kernel may be slightly different due to the position change, causing error; however, the error caused by this fact is small enough to be neglected in terms of dose distribution since the magnitude of this position change is relatively small. In



the case of significant motion, such as lung tumor motion, where kernel change due to location change may possibly cause large errors, gating technique can be used so that treatment plan does not need to be changed at all.

### ***3.6 Treatment scheme in IMRT***

EGRT can be implemented in any radiation therapy modality wherever tumor tracking is involved, such as IMRT and tomotherapy. In this work, the IMRT treatment is mainly investigated and the tomotherapy treatment will be briefly discussed. Based on the proposed tumor localization and treatment modification algorithms, the treatment scheme of EGRT is summarized to be shown in Figure 10. The treatment scheme is mainly composed of two parts, which are tumor localization and dose delivery. The delivery part relies on the localization part to provide the tumor position change information for modifying the treatment plan. In dose delivery part, based on the information of CTV, rather than PTV since margin is no longer needed in EGRT to account for the tumor uncertainties, a typical IMRT treatment plan could be made to treat the tumor. However, this treatment plan is made only for the planned tumor position. Once the tumor position shifts, it cannot be directly applied for delivery. So right before dose delivery, the tumor localization part will be called to determine the location change. With the location shift determined from the planned position, the planning will be modified accordingly using the proposed treatment modification algorithm. Depending on how fast the motion is, different sliding time windows can be used to update the tumor location. For tumors such as lung tumor which shows fast motion, relatively small time window such as sub-second time window can be used in order to monitor the tumor motion in almost real time. With both parts, a clinically acceptable IMRT treatment that is planned for CTV can be achieved with few or even no margins added.

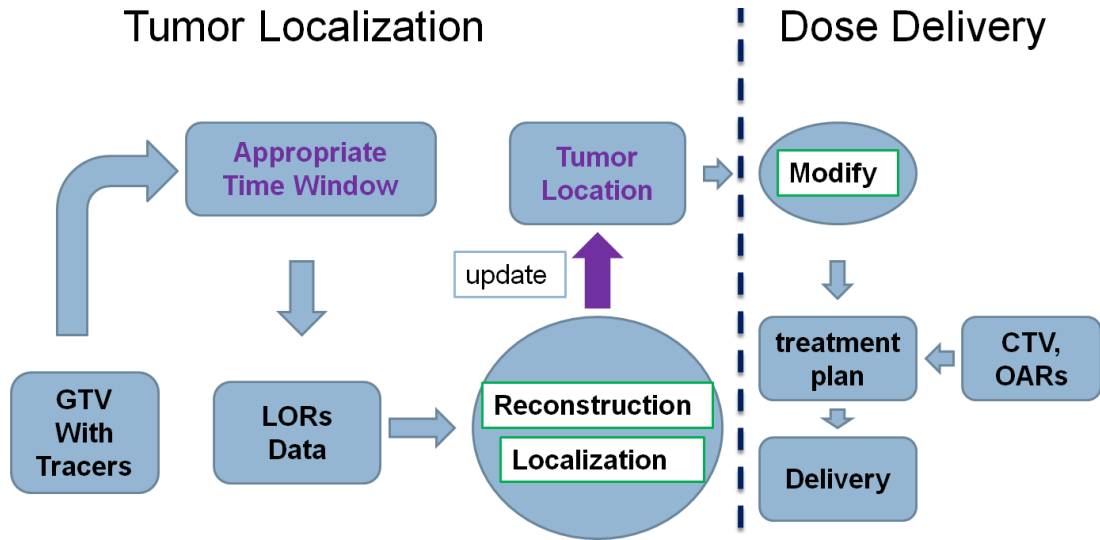


**Figure 10:** A summary of EGRT treatment scheme. The treatment scheme is composed of two parts: tumor localization and dose delivery. The updated tumor location obtained by reconstruction and localization algorithms will be used to modify the treatment plan to finally achieve a successful treatment.

With the proposed system design and corresponding treatment scheme, two essential questions need to be answered in order to validate the EGRT concept. One is to determine whether the EGRT system can achieve sufficiently high locating accuracy; the other is to verify whether using our proposed treatment plan modification algorithm, the treatment performance, i.e. the planned conformal dose distribution, can be maintained or improved.

### 3.7 Evaluation

#### 3.7.1 Overview

In order to validate the EGRT concept and its treatment scheme, we develop the following method to evaluate the EGRT performance, shown in Figure 11.

As shown, our proposed method of evaluation is also accordingly divided into two parts, based on the EGRT treatment scheme, which both start from XCAT Phantom. The XCAT Phantom provides a set of two phantoms with the same parameters and anatomy at the same time, which is an attenuation phantom and an activity phantom.

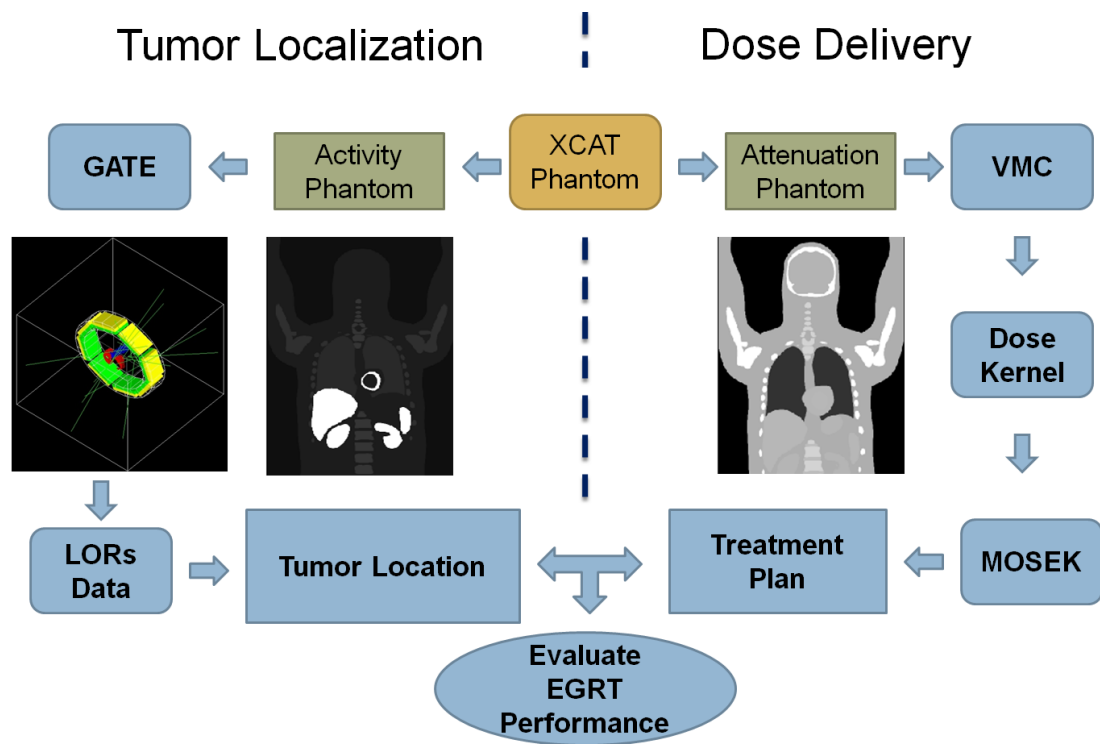


**Figure 11:** A chart flow of method evaluation. The method evaluation is also divided into two parts similarly and used to simulate the whole process of treatment scheme of EGRT.

These two phantoms have different simulation purpose in the EGRT concept. The activity phantom will simulate how the radioactive tracers will be distributed among the patient and thus is used to locate tumor through the GATE simulation. The attenuation phantom will simulate how the Linac will deposit dose in the patient and what the dose distribution will be for the tumor and normal tissue. The voxel size of the activity phantom is much smaller than the attenuation phantom and is set to be 0.98 mm by 0.98 mm by 2.5 mm. With a smaller voxel size, the tumor can be located with a higher accuracy.

The activity phantom is to be read in by GATE, a GEANT4 based dedicated Monte Carlo simulation tool for positron emission. The GATE output LORs Data, which is used to determine the tumor location. The tumor can be both static and fast moving. XCAT Phantom also generates an attenuation phantom which is to be read in by VMC, a voxel-based monte carlo simulation package. VMC will output the dose kernel to be read in by MOSEK, which is an optimization package. This package is mainly used to generate the treatment plan for the simulated phantom. With both the treatment plan and tumor location, we are able to evaluate EGRT performance. To save computation in the MC simulation of the dose distribution, the voxel size of the XCAT attenuation phantom is set to be 3.92 mm by 3.92 mm by 2.5 mm.

### **3.7.2 Reconstruction and localization**

For reconstruction in this work, we use a universal 3D parallel beam reconstruction algorithm. The reconstruction resolution is determined and optimized based on the detector size and phantom voxel size. In this work, the reconstruction resolution is 0.98mm by 0.98mm by 2.5mm. The step of interpolation of localization algorithm used in this work is 0.1 voxel in each direction.

### 3.7.3 Two simulation cases

In order to evaluate EGRT performance and validate EGRT concept, two simulation cases, pancreas tumor case and lung tumor case, have been investigated. The purpose of simulating pancreas tumor case is three fold. One is to investigate whether the tumor can be located using partial detector coverage and how the detector coverage will influence the locating accuracy. To do this, various angles are investigated based on the proposed algorithms. One is to find out whether high background signal will affect the tumor locating accuracy. Another is to validate that the setup error can be detected using the proposed PET detector arrangements so that the setup margin can be significantly reduced. For lung tumor case, the purpose is mainly to find out what temporal resolution can be achieved in detecting moving tumor, addressing the challenge of fast motion detection ability, to ensure that the periodic motion actually can be detected in almost real time in EGRT so that the motion margin can also be remarkably reduced. To do this, a lot of simulations are needed to be carried out to find out the best temporal resolution when tumor size, activity level and uptake ratio are given.

Due to various reasons, IMRT is a good choice for treating pancreas tumor because of highly conformal dose distribution. Two of many difficulties for treating pancreatic cancer are the setup error and motion indirectly caused by respiratory motion, for which large margins have to be added to compensate. Large margins can be decomposed into two parts, which are **setup margin** to compensate for the setup error, and **motion margin** to compensate for the motion issue. However, in this work, the pancreas case is used to mainly to validate that setup margin can be reduced using EGRT with an assumption that tumor motion can be neglected. The motion issue will be discussed and resolved in lung tumor case in which motion issue is the main source for margins.

Figure 12 shows the one set of two phantoms generated for simulation and the

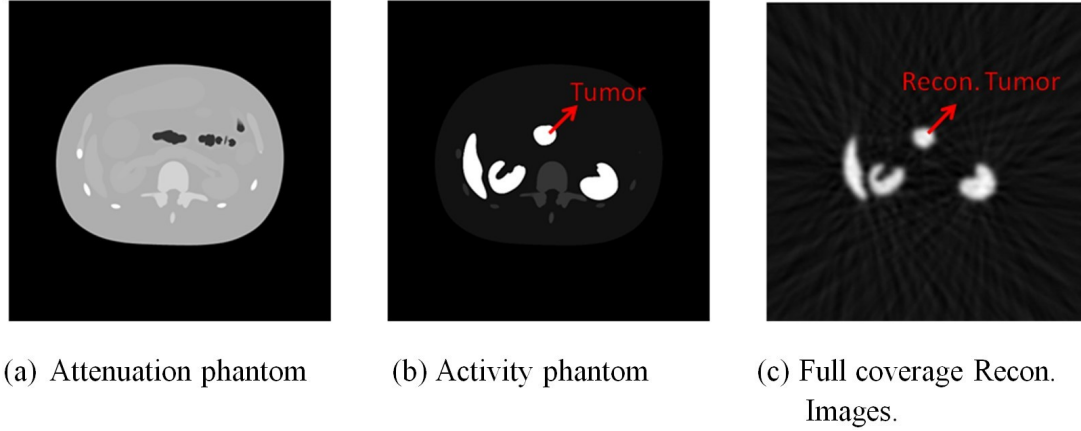


**Figure 12:** The XCAT phantom images of pancreas tumor case and its reconstructed tumor images.

self-made tumor which only is shown in activity phantom. This self-made tumor has the same uptake ratio as other organs such as left kidney, right kidney and liver. The left kidney, right kidney, spinal cord and small bowel are taken as critical structures for IMRT planning according to routine clinical practice.

For the pancreas tumor, 10 fields were used at angles of  $270^\circ$ ,  $300^\circ$ ,  $330^\circ$ ,  $0^\circ$ ,  $25^\circ$ ,  $55^\circ$ ,  $85^\circ$ ,  $115^\circ$ ,  $145^\circ$ ,  $175^\circ$  based on a standard clinical protocol[11]. Each field targeted the center of PTV, and contained 21 by 17 beamlets, with a beamlet size of 5 mm by 5 mm at the source-to-axis distance (SAD). Uptake ratio of tumor over general background is set to be 8:1. A set up error of 1.176cm in lateral direction and 1.176cm in superior direction is simulated.

Currently in IMRT clinical practice, the biggest problem associated with the lung cancer is the respiratory motion. EGRT is a good choice for tumor motion issue. And the main purpose of simulating the lung tumor case is to prove that the motion margin can be reduced because EGRT can track the tumor almost in real time, even with partial PET detector coverage. Figure 13 shows the one set of two phantoms generated for simulation and the self-made tumor which is shown in both attenuation and activity phantom. This self-made tumor has a 15:1 uptake ratio over surrounding tissues. The left lung, right lung, spinal cord and heart are taken as critical structures

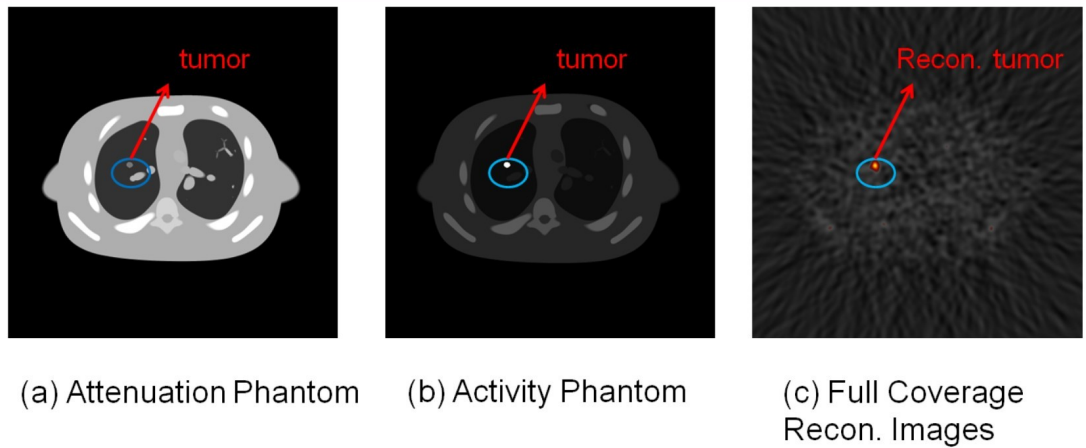


**Figure 13:** The XCAT phantom images of lung tumor case and its reconstructed tumor images.

for IMRT planning according to routine clinical practice.

For the lung tumor case, five fields were used at angles of  $70^\circ$ ,  $115^\circ$ ,  $195^\circ$ ,  $230^\circ$ ,  $270^\circ$  based on a standard clinical protocol[7]. Each field targeted the center of PTV, and contained 21 by 17 beamlets, with a beamlet size of 5 mm by 5 mm at the SAD. Uptake ratio of tumor over general background is set to be 15:1. Since it is generally accepted that the respiratory motion is a periodic motion, we simulate a half-sine-wave motion in the posterior-anterior direction, with a magnitude of 1.96 cm. The respiratory cycle is set to be 5 seconds divided into 15 phases, resulting in a temporal resolution of 0.33 s.

### 3.8 Results

#### 3.8.1 Pancreas tumor case

As shown in Figure 12 (c), with full detector coverage, the tumor can be easily identified in reconstructed images. With our proposed algorithm, it is found out that for full coverage, the position locating accuracy is about 0.8 mm. However, like mentioned before, there is no full PET detector coverage so that it is very important to find out how the locating accuracy change with decreasing coverage. The reconstructed images for three selected angles which are  $240^\circ$ ,  $180^\circ$  and  $120^\circ$  for two different detector

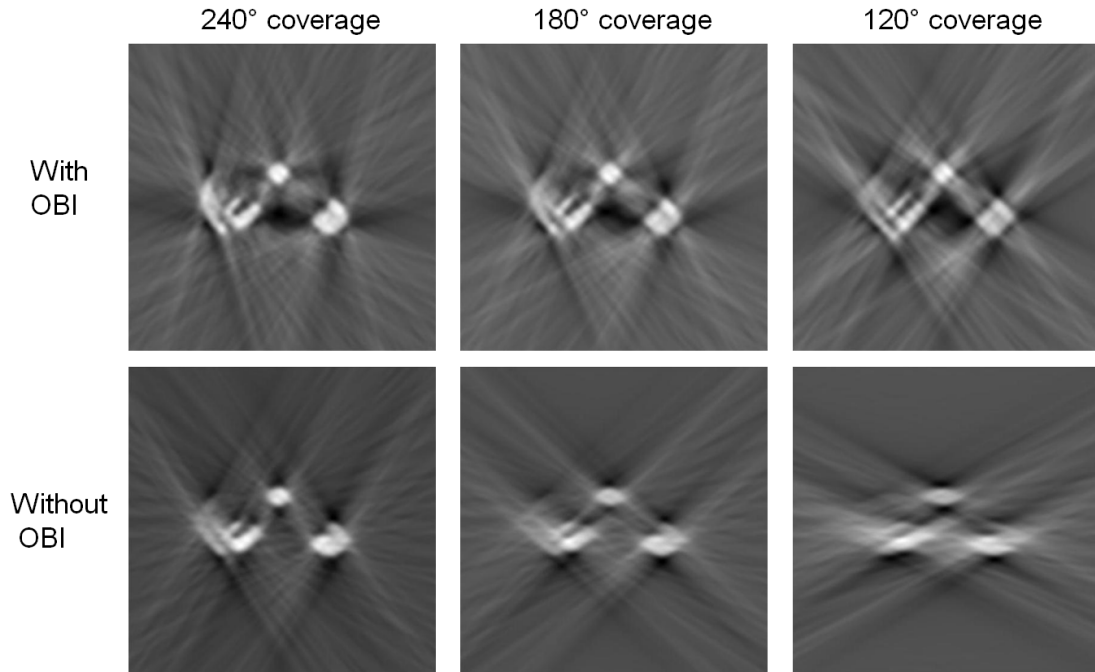


**Figure 14:** The reconstructed images of pancreas tumor case with specific angle coverage of 240°, 180° and 120°.

arrangements are shown in Figure 14. The result of locating accuracy for different detector coverages is shown in Figure 15.

As expected, system with OBI arrangement has better locating accuracy for the same angle coverage. It is found out that with approximate 150 degree, EGRT should be able locate the tumor with an accuracy of about 1.2 mm, which is sufficiently accurate according to clinical criteria.

As shown in Figure 16, if there is setup error, the planned dose distribution will miss the CTV and lead to unacceptable dose distribution. That is why typically a setup margin needed to be added to CTV. Note that the prescribed dose is normalized to be  $10^{-3}$ . The same thing applies to other DVH figures.

However, as shown in Figure 17, with EGRT, before radiation delivery, the setup error will be detected and thus the treatment plan can be modified accordingly so that the radiation will hit the tumor as the tumor is in the planned position and thus generate a satisfied dose distribution. The modification of treatment plan, i.e. how



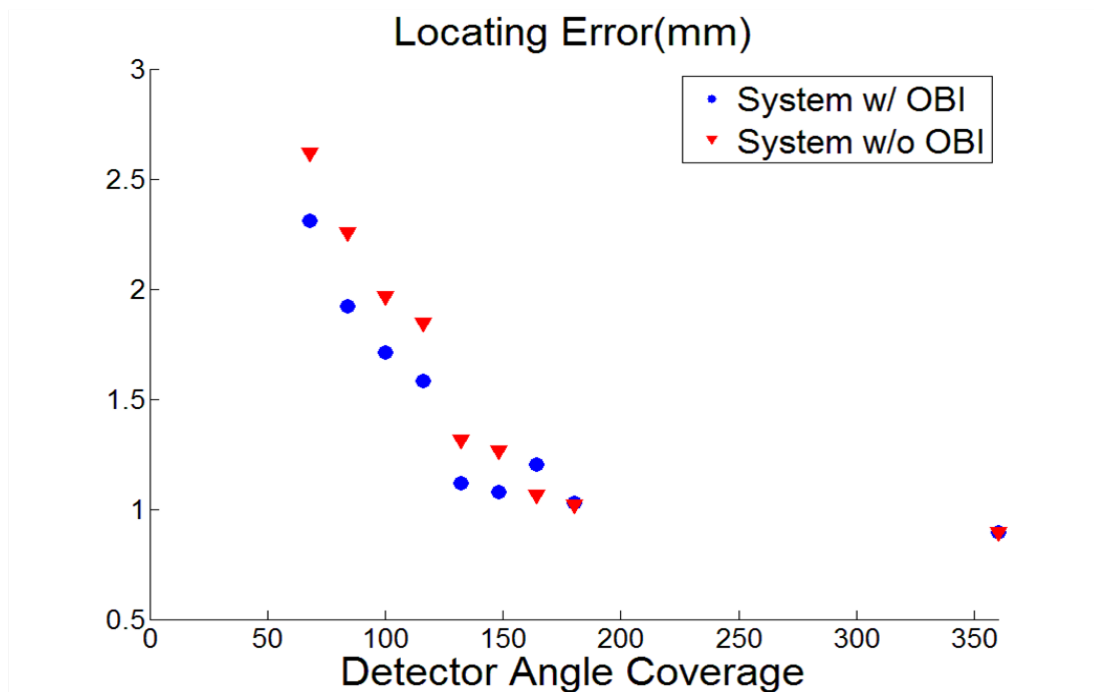


**Figure 15:** The locating accuracy of different detector angle coverage for both arrangements.

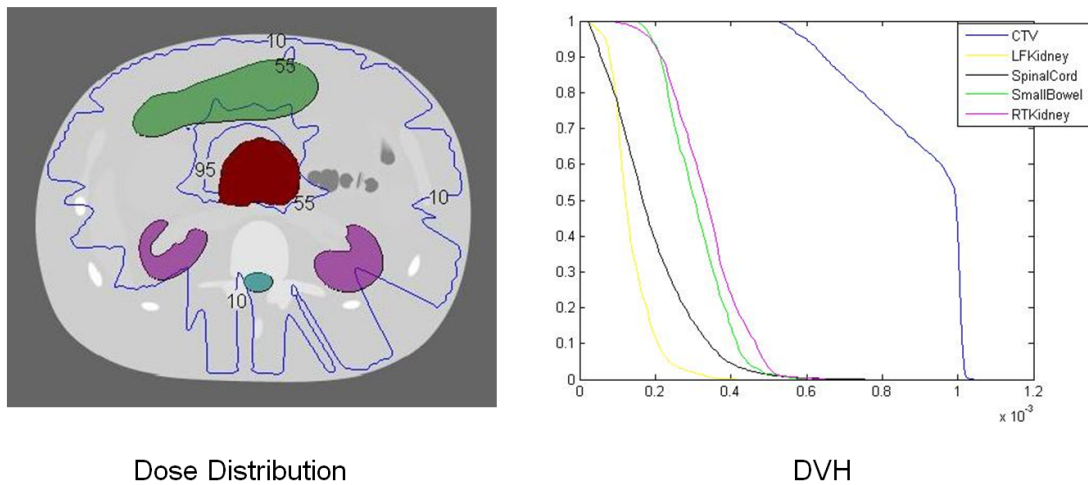


**Figure 16:** The dose distribution and DVH for pancreas tumor case if setup error exists without EGRT. The tumor is in red color; other colored organs are the organs at risk.

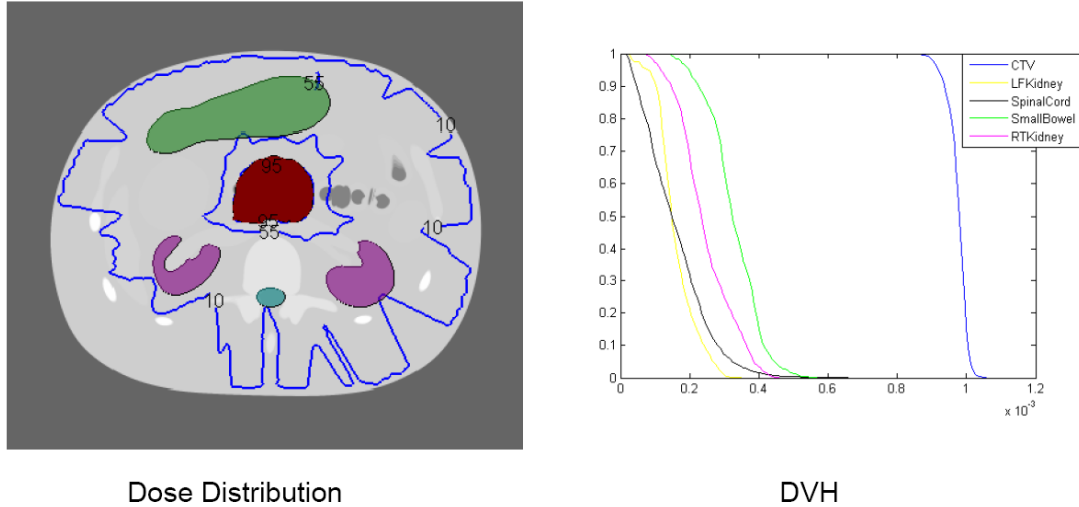


**Figure 17:** The dose distribution and DVH for pancreas tumor case if setup error exists with EGRT. The tumor is in red color; other colored organs are the organs at risk.

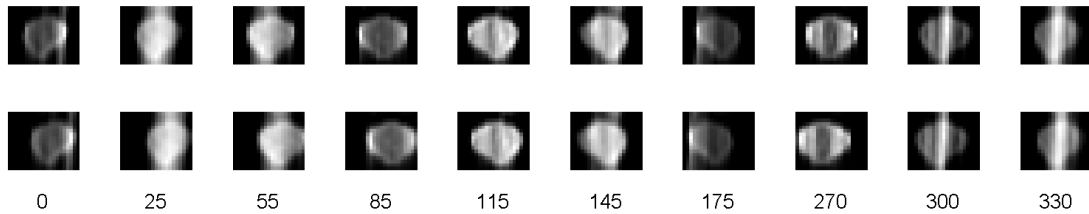


**Figure 18:** Fluence map modification. Upper: before modification; lower: after modification. The numbers indicate the field angles.

the treatment plan is shifted, is shown in Figure 18.

### 3.8.2 Lung tumor case

As shown in Figure 13(c), with full detector coverage, the tumor can be seen from reconstructed images. The comparison of the detected motion and the simulated motion is shown in Figure 19.(a) , with the error of detection shown in Figure 19 (b). The result indicates an average error of about 2 mm.

For 150 degree coverage, an averaged error of about 3 mm is observed. The comparison of simulated motion and detected motion and error of detection is shown in Figure 20.

The dose is delivered the similar way as gating technique, which means the dose is

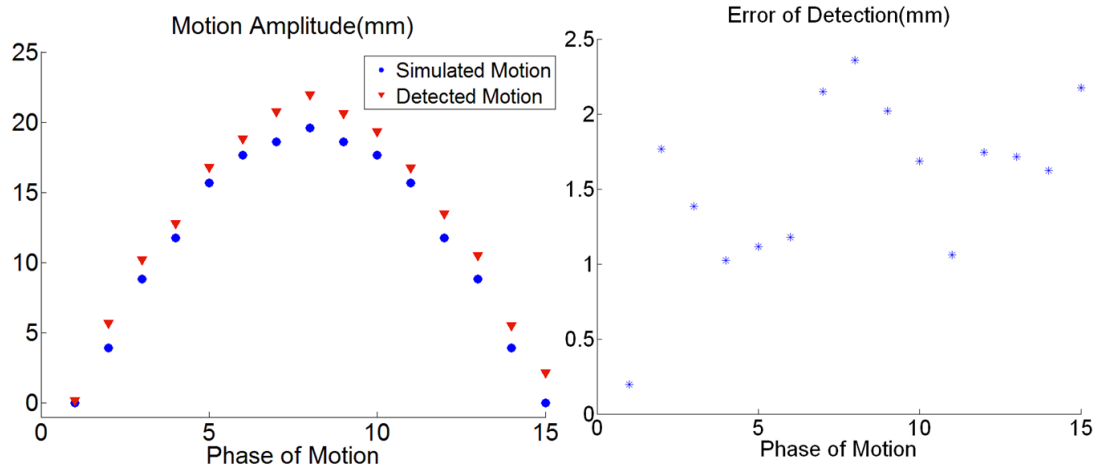


**Figure 19:** The locating accuracy of lung tumor case for full detector coverage.

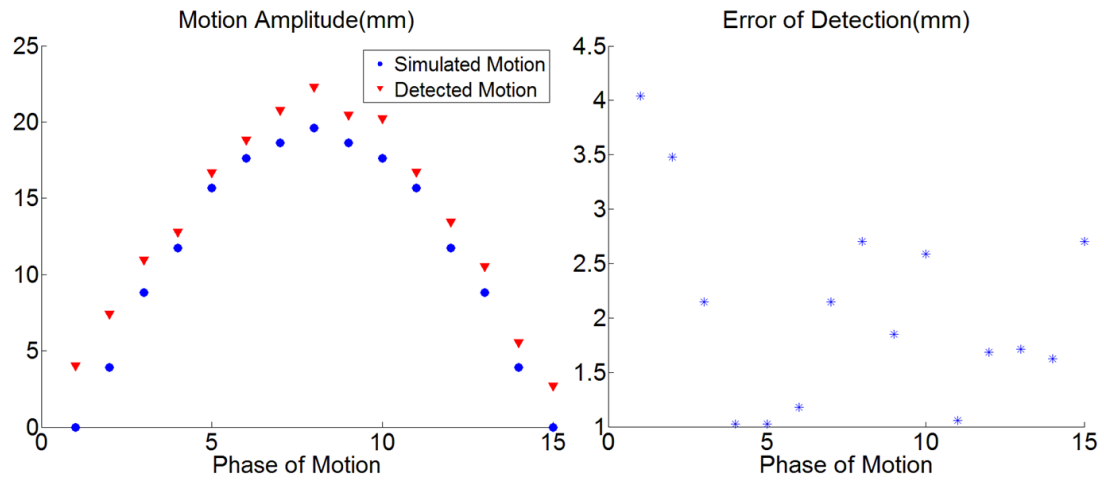


**Figure 20:** The locating accuracy of lung tumor case for 150 degree coverage.

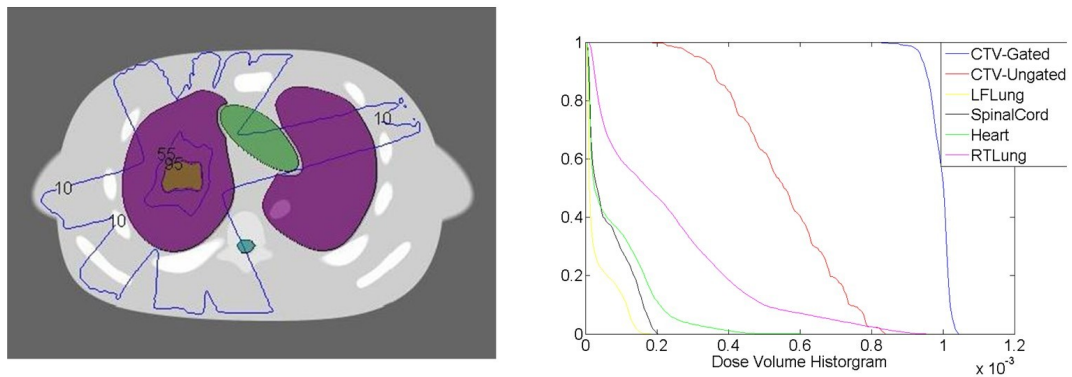


**Figure 21:** The dose distribution and DVH for lung tumor case if setup error exists with EGRT based on gating delivering technique. The tumor is yellow color; other colored organs are the organs at risk.

delivered only in certain position such as base phase position. The dose distribution is shown in Figure 21. It can be seen that with EGRT, the margin can be significantly reduced while still maintaining a highly conformal dose distribution. For un-gated dose delivery, which is simulated by delivering the dose equally among all the phases, the dose distribution is not acceptable.

## CHAPTER IV

### EGRT IN TOMOTHERAPY

#### *4.1 Overview*

In tomotherapy scheme, the two key issues, tumor tracking and treatment plan modification still apply. That is, in the tomotherapy scheme, there are also two algorithmic difficulties in the detailed implementation. The first is how to locate the 3D location of the tumor in real time from the detected LORs. The second is how to deliver the dose based on the acquired tumor location information and an existing treatment plan. The scope of this simulation is to demonstrate the concept of EGRT and to provide viable solutions to the two challenges above. Another purpose of this simulating case is to validate the EGRT concept in the tomotherapy scheme and get a preliminary result.

However, since dose is delivered slice by slice in tomotherapy scheme, there are some differences between tomotherapy scheme and IMRT scheme. In tomotherapy, treatment is done for all angles and full sinogram is available because linac is rotating fast. Also, the Linac responds to individual LOR and the dose is delivered to one LOR rather than to one field. As mentioned in previous chapter, the main content in this chapter will focus on how to validate the EGRT concept in tomotherapy scheme.

#### *4.2 Proposed EGRT tomotherapy system design*

As discussed before, EGRT system mainly consists of a typical Linac for radiation delivery and PET detectors for tumor localization. They are mounted together in the same gantry such that the EGRT system can do tumor tracking to get the tumor position and simultaneously deliver the radiation precisely with the help of real-time

tumor location. This is quite different from the PET-guided radiation therapy which takes quite a long time to acquire PET images before the radiation delivery and the tumor tracking is not being done concurrently with the treatment. A schematic diagram of EGRT system for tomotherapy scheme is shown in Figure 22.

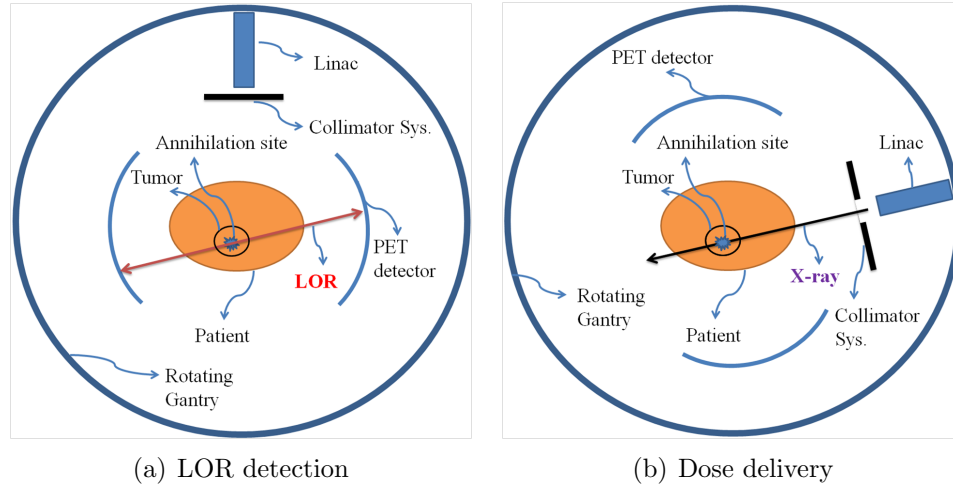


**Figure 22:** The schematic diagram of the proposed EGRT system for tomotherapy scheme. Left: one coincidence event is detected; Right: The linac has been rotated to align with this LOR within a very short time and simultaneously delivers the radiation along this LOR.

In EGRT tomotherapy scheme, after the positron emitter injected into patient, the gamma-ray detectors as used in a PET scanner detect the LORs generated by positron events. Once the positron event is determined to be inside the tumor target based on the uptake ratio and the treatment plan, the corresponding LOR will be enqueued into a list of beamlets waiting for dose delivery. At the first time when the rotating Linac meets the enqueued LOR, radiation will be delivered along the LOR passing through the target.

### 4.3 *Planning sinogram, emission sinogram and treatment plan modification*

It is very useful to apply the concept of sinogram in EGRT. Some examples of sinograms are shown in Figure 23. Planning sinogram is obtained by converting the

planned dose data, which is obtained by optimization, from the 1D matrix into a 2D matrix with a particular size. In this work, 3600 beam around the phantom has been used to deliver the dose. 3600 beams are composed of 180 fields and each field has 20 lateral beams. Therefore, the planning sinogram will have a size of 180 by 20. Thus, each grid of the sinogram corresponds to one unique beam position among all the 3600 beams. The intensity of each grid is the planned dose for the corresponding beam position.

Each LOR can be represented uniquely by a data pair of the angle of the line and its displacement from origin. GATE outputs the position of two ending point of LOR. This data output can be converted into the Emission sinogram, each grid of which also signifies one beam position. Note that the displacements are converted into the sequence number of the 20 beamlets. In this case, the size of the Emission sinogram is intentionally made the same with the planning sinogram and thus the grids of Emission sinogram coincide with those in planning sinogram in terms of beam positions. The main difference is that the intensity of Emission sinogram is the number of coincidence counts received in the beam positions indicated by grid position. When performing treatment, we expect to deliver the planned dose in each grid of planning sinogram according to the number of counts in the corresponding grid of Emission sinogram.

Actually, Figure 23 also shows how we can get the location of the tumor and how we should modify the treatment plan based on the tumor location information. As shown, in emission sinogram, if there is no setup error, the sino-curve of the tumor will be almost a straight line; however, if there is setup error, that is, the tumor shifts from its original location, the sino-curve of the tumor will be a sinusoidal curve rather than a straight line. From the phase and the amplitude of this curve, the tumor position change can be determined. Then, the same shift amount of the emission sinogram can be applied to planning sinogram. This is how we modify the treatment plan in

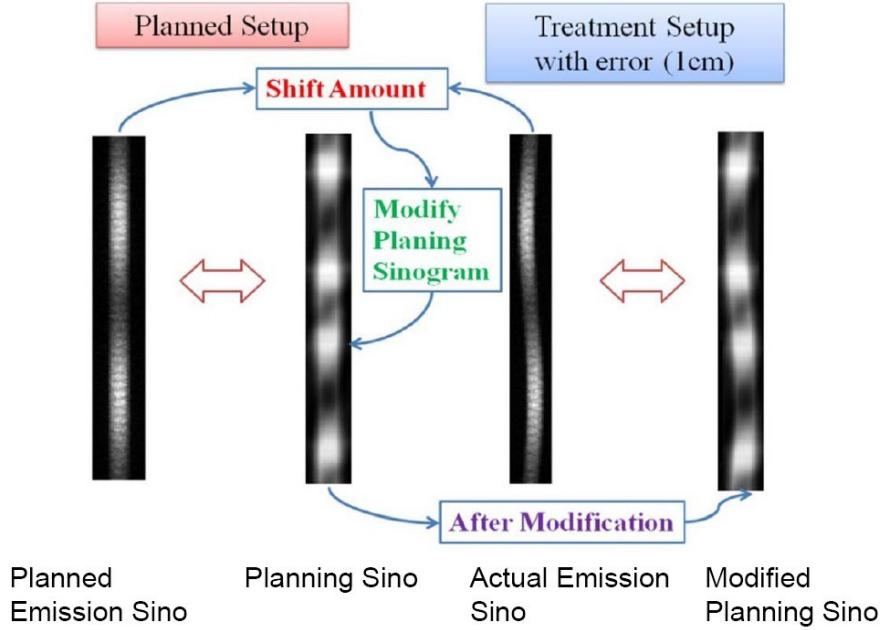


**Figure 23:** Sinograms involved in simulations to demonstrate concept of treatment without using margins. Emission sinogram will be shifted if error exists, then we can modify the planning sinogram according to the shift amount of Emission sinogram.

tomotherapy scheme.

#### 4.4 Adaptive dose delivery

Suppose we have obtained a complete sinogram set, including a Emission sinogram and the corresponding planning sinogram. Imagine a particular grid, by looking up Emission sinogram, we get the number of coincidence counts in this grid is  $P$ ; by looking up planning sinogram, we know the intensity to be delivered for the position corresponding to this grid is  $I$ . So, for each count, the intensity to be delivered shall be:

$$I_0 = \frac{I}{P}.$$

By delivering dose equally among all the detected LORs, the error of dose delivery will be minimized. We are able to deliver the planned dose completely if:

- we have enough counts during the treatment;
- we know the complete Emission sinogram before the treatment.



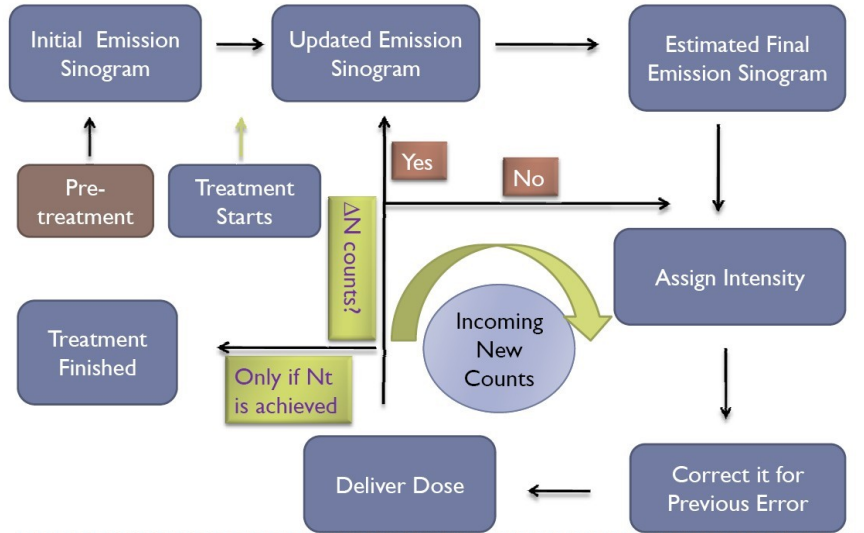


**Figure 24:** Adaptive dose delivery of EGRT tomotherapy.

For the first condition, it will be achieved with a reasonably long treatment time; as for the second one, it is impossible to be met because we are responding to each individual LOR from the beginning to the end of treatment and thus we are doing treatment in real time and therefore the Emission sinogram is formed dynamically. However, this problem can be solved using our proposed adaptive dose delivery scheme.

Before treatment starts, we do a pre-treatment to obtain one initial Emission sinogram to be updated from. Then we can continuously update the Emission sinogram with incoming new counts. We estimate the final Emission sinogram from the updated Emission sinogram. Then we assign the dose for each count according to the estimated Emission sinogram and compensate for previous errors simultaneously before delivery since the estimated Emission sinogram is always noisy. With more and more counts coming in, the estimated final Emission sinogram will be more and more precise and the error will, ideally, converge to zero. When the number of treatment counts is reached, the treatment is finished and the planned dose is delivered completely. The optimized dose distribution and DVH will be achieved with negligible errors. The adaptive dose delivery workflow is shown in Figure 24. For how to compensation for previous error, it is shown in Figure 25.

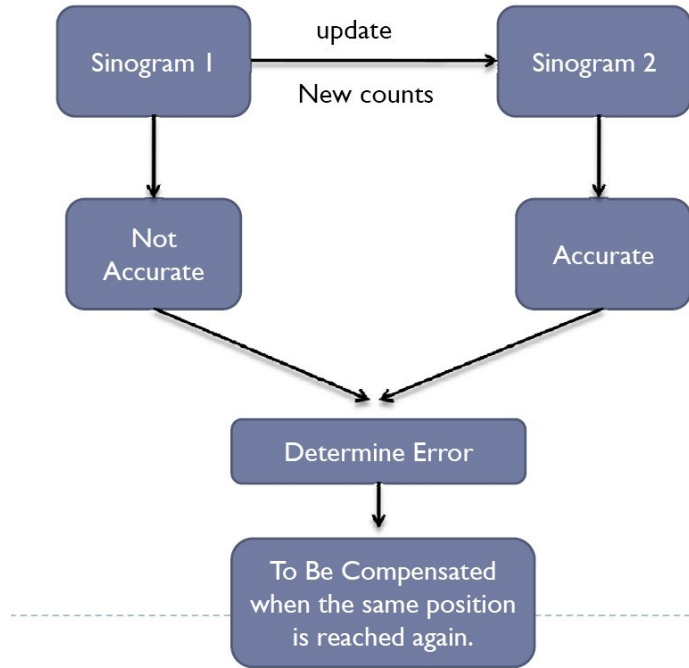


**Figure 25:** Compensation method in adaptive dose delivery.

#### ***4.5 Treatment scheme in tomotherapy***

Different therapy scheme may have different treatment scheme, although the concept of EGRT is the same. For tomotherapy scheme, the treatment scheme is shown in Figure 26. The treatment scheme of EGRT tomotherapy starts from injecting radioactive tracers into GTV and the LORs data can be obtained to be input into the adaptive dose delivery module to achieve a successful treatment. The core part of EGRT tomotherapy is the adaptive dose delivery method and treatment plan modification if tumor position change is detected.

#### ***4.6 Evaluation***

##### **4.6.1 Overview**

The workflow is illustrated in Figure 27. Since the EGRT system typically contains two main components, i.e. Linac and PET detector, the workflow has two separate paths of simulation, which converge in the end to achieve successful treatment

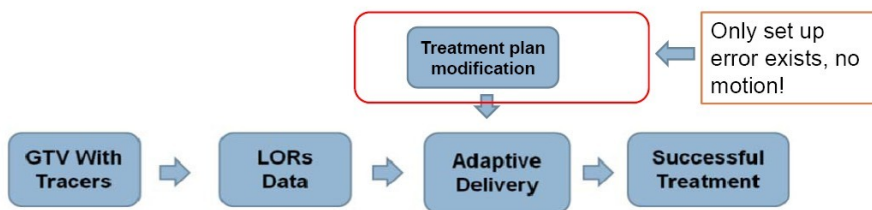


**Figure 26:** Treatment scheme of EGRT tomotherapy.

using proposed adaptive dose delivery algorithm. Starting from the same phantom geometry, the left side path first calculates the dose kernel, which is the dose distribution achieved by beamlets with unit intensity, via VMC++, then computes the planned dose for all simulated beamlets positions via optimization, finally rearranges the planned dose data into **planning sinogram**; the right side path first simulates the emission process using GATE package and output the coincidence counts data, then convert the data into **Emission sinogram**. Using the two sinograms together, we expect to deliver exactly the prescribed dose to the phantom via proposed adaptive dose delivery scheme and achieve a desired dose distribution.

#### 4.6.2 Geometry of evaluation phantom

The geometry of simulated prostate cancer phantom is shown in Figure 28(a). The human body is simulated using an ellipse with a major and minor semi-axis of 18 and 12 cm respectively. PTV and organs at risk (OARs) are circles with a radius of 3 cm for PTV, 2.5 cm for rectum and 2 cm for other OARs (bladder, left femoral head and right femoral head). Conventionally, for IMRT, the treatment planning is done at five fixed angles. In our simulation, the treatment planning is done every other degree over 360 degrees since this is a tomotherapy scheme. This means a total of 180 angle positions where source can be placed. At each source position, the width of X-ray is specified using 20 beamlets, each of which has a size of 5mm by 5mm

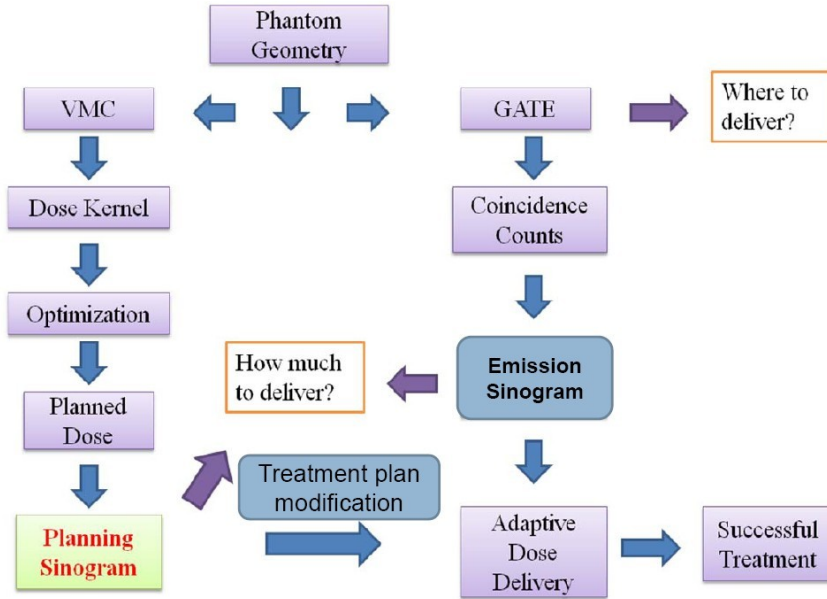
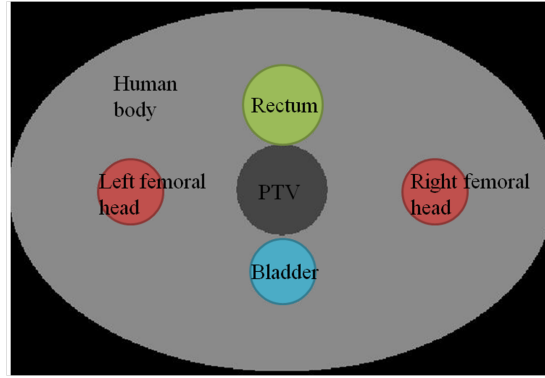


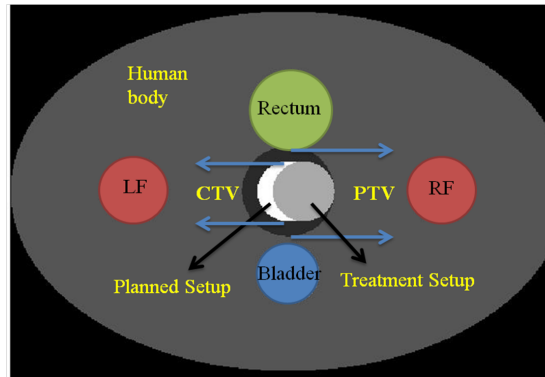
**Figure 27:** Method of Evaluation for EGRT Tomotherapy.

at the SAD. These 20 beamlets are arranged in one line with a total length of 10 cm and their common center is placed in the midpoint of source-to-origin line which is perpendicular to beamlets line. Since the source is placed sufficiently far from the phantom, the beams going through the beamlets can be approximately viewed as parallel beams. The total coverage of X-ray for each source position is 10 cm, covering the whole PTV region. Therefore, with 180 source positions and 20 beamlets for each source position, we have 3600 possible different beams in total to deliver the dose for each slice.

The geometry of treatment without using margins is shown in Figure 28(b). The original PTV's radius is 3 cm and we assume the margin is 1 cm which makes the CTV's radius 2 cm. **Planned setup** means CTV is at the phantom center. **Treatment setup** means CTV is some distance, in our simulation set to be 1 cm which is just the margin value, deviated from the planned setup.



(a) Geometry of prostate cancer phantom



(b) Geometry for treatment without using margins

**Figure 28:** Geometry involved in simulations.

### 4.6.3 Optimization

The goal of optimization is to determine the planned dose intensity for all the 3600 possible beams so that the PTV and OARs will achieve the desired dose distribution and dose volume histogram (DVH) if the planned dose for each beam position is delivered. In our simulation, the prescribed dose for PTV is set to be  $10^{-3}$  for the consideration of convenience, while for other OARs it is set to be a sufficiently low value. The optimization is done using MOSEK package. The main output of the optimization is the planned dose intensity for all 3600 beams. A typical optimized DVH is shown in Figure 30(c).

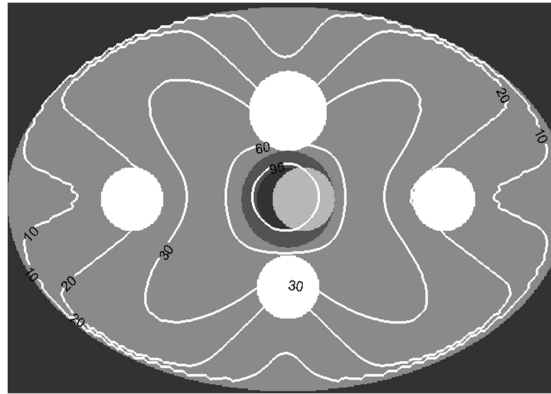
#### 4.6.4 Concept of treatment without margins

Previously, we are treating PTV rather than CTV. The PTV is composed of CTV plus margins. The reason why we use safety margins (typically 1 to 2 cm in lung cancer) is because of tumor motion or patient setup error. This leads to increased dose to normal tissues surrounding CTV. In EGRT tomotherapy, since Emission sinogram can tell the position of the tumor from the sinogram itself, margins are no longer needed. The case of patient setup error is simulated. Emission sinogram will indicate whether there is setup error in process of real-time therapy. As shown in Figure 23, if there is setup error, Emission sinogram will look like (c) rather than (a). That is, the Emission sinogram is shifted because of position change. However, planning sinogram is based on the planned setup position and unaware of setup error. Thus it cannot be directly applied for dose delivery. However, from Emission sinogram, we know the position change of CTV so that we can modify the planning sinogram according to that particular change.

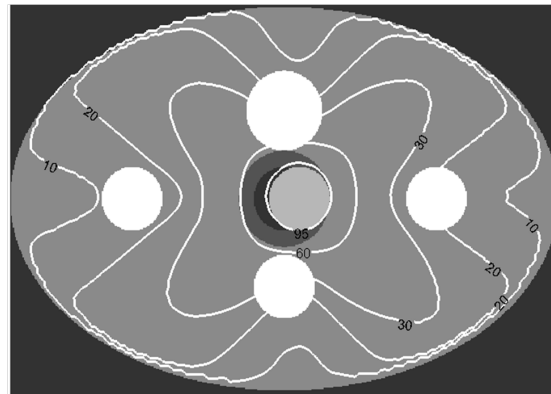
As shown in Figure 28(b), if the CTV is at the planned setup position, which is in the phantom center, the Emission sinogram is a straight line. If the CTV is set up incorrectly, which means the CTV is shifted some distance from the phantom center, the Emission sinogram is a sinusoidal curve, shifted from the straight line because of the position change. We can perform the same amount of shift of the Emission sinogram on the planning sinogram to obtain the modified planning sinogram. Because the CTV deviates not so far from its planned setup position, we can assume this modified planning sinogram approximated equals the optimized sinogram for the current treatment setup. And this assumption is validated in our simulation by generating dose distribution and the error turns out to be negligible.

## 4.7 Results

This section show two important results about this study: dose distribution and DVH. Dose distribution is shown in Figure 29 and DVH is shown in Figure 30. From Figure 29, it can be seen that even the tumor shifts from its planned position, the radiation is still able to locate it with the help of emission guidance and then achieve a satisfied dose distribution. This can be further verified by DVH shown in Figure 30.

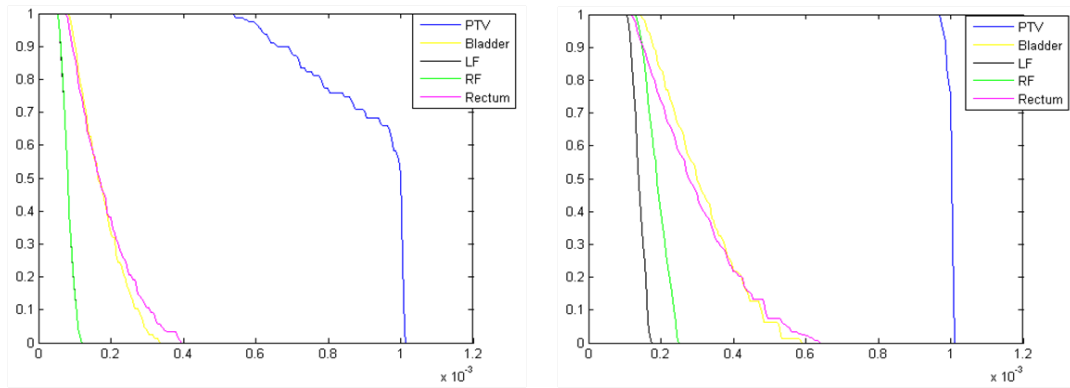


(a) DVH for treatment setup using unmodified sinogram

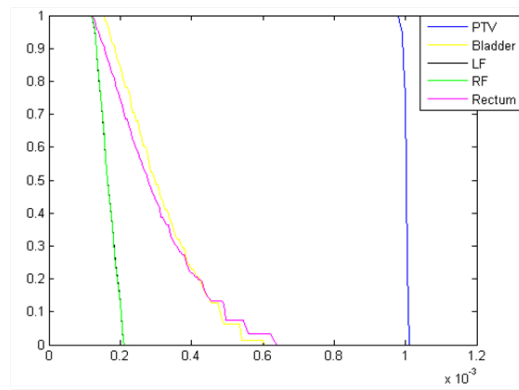


(b) DVH for treatment using modified sinogram

**Figure 29:** Dose distribution of treatment without using margins. The number on iso-dose line is the percentage of prescribed dose. Geometry is the same as Figure 28(b). Left: dose distribution without any method if setup error exists, corresponding to Figure 30(a). Right: dose distribution using proposed method even if setup error exists, corresponding to Figure 30(b).



(a) DVH for treatment setup using unmodified sinogram (b) DVH for treatment using modified sinogram



(c) optimized DVH for planned setup

**Figure 30:** DVHs of treatment without using margins.



## CHAPTER V

### DISCUSSION, CONCLUSION AND FUTURE WORK

#### *5.1 Discussion and conclusion*

Our preliminary simulation results indicate that EGRT is able to deliver conformal dose distribution to both shifted stationary tumor and fast moving tumor by tracking the tumor position accurately. One of the biggest advantages of emission guidance is that the margins for compensating uncertainties that are routinely used will be significantly reduced or even completely eliminated. This is validated through our simulations. However, treatment without margin is not the sole clinical benefit or may not even be the most important one of EGRT. EGRT is able to provide further useful information that may affect the future development of the radiation therapy of cancer. For example, EGRT is able to distinguish the active part of tumor and the dead part, allowing the research of biological treatment planning.

In this work, EGRT can be further improved to exhibit more accurate and powerful guidance by enhancing the proposed algorithms in several aspects. First, the current reconstruction algorithm used is simple parallel beam reconstruction. All the oblique LORs, about 90 percent of total LORs data, are wasted, degrading the temporal resolution and increasing the data noise. Furthermore, the localization algorithm can also be improved. One way is to optimize the interpolation parameters which have an influence on the locating accuracy. Another way is to introduce weighting factors into localization process, since currently every voxel of the tumor is weighted equally. However, the inner tumor voxels has more influence to determine the tumor location for current localization algorithm and therefore deserves higher weighting factors than the outer tumor voxels. Also, current simulation assumes that the detector is not

rotating at all to loosen the hardware constraints. However, this may not be the case because the linac is rotating between different fields and PET detectors will also be rotating. In that case, sinogram data can be made complete if an estimation algorithm based on prior information is well established.

Although with the proved feasibility, there are some issues needed to be addressed. One of the main challenges comes from the dose caused by radioactive tracers. Through our investigation, this nuclear medicine dose will not be a big issue due to the fact that the dose caused by one-time injection of radioactive tracers is actually significantly less than one-time cone beam CT (CBCT) imaging. Plus, there are potentially several methods of reducing the nuclear medicine dose in detailed EGRT implementation. For example, a 4D reconstruction rather than simple parallel beam reconstruction should be implemented so that the data will be used more efficiently, meaning that only smaller activity is needed or lower dose rate can be used. Or shortening the time of therapy will further reduce the activity that is needed. Another possible method will be to do a regional reconstruction so that not only the locating accuracy will be improved but also the events needed to locate the tumor will be reduced. Also, in current practice, due to increased margins, the desired radiation dose must be delivered over a series of fractions (typically 30-40, over a 5 week period) in order to minimize toxicity to healthy surrounding tissue. This will significantly increase CBCT dose, however, with EGRT, the fractions can be reduced because of very small margins or even no margins.

Another issue of EGRT will be the uptake ratio of the radioactive tracers. Current simulation indicates that the higher the uptake ratio, the easier and faster the tumor will be located. This is understandable because with higher uptake ratio, the tumor will be more easily distinguished from the background organs or tissues. Our simulation results have already proved that as long as the background organs or tissues are not physically mixed with each other, the uptake ratio issue will not disable the

algorithm. For those the tumor is immersed with the background, ideally as long as the uptake ratio is not exactly the same, the tumor should be able to be located. From our simulation experience, in order to achieve an acceptable locating accuracy, the tumor can be located with an uptake ratio about 2:1 to 10:1 for reducing setup margins, 5:1 to 15:1 for reducing motion margins. For those tumors with uptake ratio lower than 2:1, EGRT may not be suitable for them. However, most of the tumors have an uptake ratio larger than 2:1, especially for lung tumor whose motion issue is still not resolved in current radiation therapy practice. Although current work does not include the cases in which tumor may deform, EGRT is able to resolve the tumor deformation issue in the future work through some algorithm improvement.

In summary, this work has developed a set of basic algorithms to validate a new emission guided radiation therapy concept, which uses positron emission for tumor treatment guidance. This set of algorithms mainly solves the issues of tumor tracking and maintaining treatment performance by modifying the treatment plan for EGRT. High accuracy and high temporal resolution of tumor tracking can be achieved, reducing the margins and providing the tumor position change for treatment plan modification. Treatment performance can thus be maintained by modifying the treatment plan instantly and right before radiation delivery. Therefore, unlike the conventional PET-guided radiation therapy system, EGRT system is able to perform real-time tumor tracking and radiation therapy simultaneously, greatly improving the performance of current radiation therapy.

## **5.2 *Future work***

A lot of work can be done in various aspects. First of all, the localization accuracy needs to be further improved, as well as the stability of the accuracy. Temporal resolution also needs to be further increased. Although current simulation have already shown acceptable results in both locating accuracy and temporal resolution,

things may not turn out to be as perfect as those shown in simulations in practical systems. Potential problems may show up in future phototype system and clinical EGRT systems and its applications.

Moreover, tumor deformation may be a great challenge in future development of EGRT applications. Tumor deformation can be incorporated by determining possible deformation shapes which are to be used in tumor localization. Although it is ideally practical to include tumor deformation into current algorithm theme, it is still difficult to take that into account while still maintaining a sufficiently good result. Therefore, some creative and persistent work is needed here. Also, the counterpart on tomotherapy scheme is only finished partially. We have already shown that the EGRT tomotherapy scheme is able to detect the setup error; however, we are still working on the motion problem. Motion problem is more challenging for tomotherapy scheme than IMRT scheme because the tracking of tumor position is not finished until the dose is finished delivering.

The future work not only represents the challenges that lie in front of the development of EGRT, but also at the same time indicates the bright future of EGRT since once those issues are addressed, EGRT will have broad application in clinical practice and bring more patient comfort and care.

## REFERENCES

- [1] ANANTHAM, D., FELLER-KOPMAN, D., SHANMUGHAM, L., BERMAN, S., DE-CAMP, M., GANGADHARAN, S., EBERHARDT, R., HERTH, F., and ERNST, A., “Electromagnetic Navigation Bronchoscopy-Guided Fiducial Placement for Robotic Stereotactic Radiosurgery of Lung Tumors,” *Chest*, vol. 132, no. 3, p. 930, 2007.
- [2] ANDERSON, E., “The MOSEK Optimization Toolbox for MATLAB Version 2.5, Users Guide and Reference Manual,” *World Wide Web*, <http://www.mosek.com> (1999–2002).
- [3] CROOK, J., RAYMOND, Y., SALHANI, D., YANG, H., and ESCHE, B., “Prostate motion during standard radiotherapy as assessed by fiducial markers,” *Radiotherapy and Oncology*, vol. 37, no. 1, pp. 35–42, 1995.
- [4] EKBERG, L., HOLMBERG, O., WITTGREN, L., BJELKENGREN, G., and LANDBERG, T., “What margins should be added to the clinical target volume in radiotherapy treatment planning for lung cancer?,” *Radiotherapy and oncology*, vol. 48, no. 1, pp. 71–77, 1998.
- [5] EZZELL, G., GALVIN, J., LOW, D., PALTA, J., ROSEN, I., SHARPE, M., XIA, P., XIAO, Y., XING, L., and YU, C., “Guidance document on delivery, treatment planning, and clinical implementation of IMRT: Report of the IMRT subcommittee of the AAPM radiation therapy committee,” *Medical Physics*, vol. 30, p. 2089, 2003.
- [6] GALVIN, J., EZZELL, G., EISBRAUCH, A., YU, C., BUTLER, B., and OTHERS, “Implementing IMRT in clinical practice: a joint document of the American Society for Therapeutic Radiology and Oncology and the American Association of Physicists in Medicine,” *International journal of radiation oncology, biology, physics*, vol. 58, no. 5, pp. 1616–1634, 2004.
- [7] JIANG, S., POPE, C., JARRAH, K., KUNG, J., BORTFELD, T., and CHEN, G., “An experimental investigation on intra-fractional organ motion effects in lung IMRT treatments,” *Physics in Medicine and Biology*, vol. 48, p. 1773, 2003.
- [8] KAWRAKOW, I., “Improved modeling of multiple scattering in the Voxel Monte Carlo model,” *Medical Physics*, vol. 24, p. 505, 1997.
- [9] KAWRAKOW, I., FIPPEL, M., and FRIEDRICH, K., “3D electron dose calculation using a voxel based Monte Carlo algorithm (VMC),” *Medical physics*, vol. 23, p. 445, 1996.

- [10] KUPELIAN, P., WILLOUGHBY, T., MAHADEVAN, A., DJEMIL, T., WEINSTEIN, G., JANI, S., ENKE, C., SOLBERG, T., FLORES, N., LIU, D., and OTHERS, “Multi-institutional clinical experience with the Calypso System in localization and continuous, real-time monitoring of the prostate gland during external radiotherapy,” *International journal of radiation oncology, biology, physics*, vol. 67, no. 4, pp. 1088–1098, 2007.
- [11] LANDRY, J., YANG, G., TING, J., STALEY, C., TORRES, W., ESIASHVILI, N., and DAVIS, L., “Treatment of pancreatic cancer tumors with intensity-modulated radiation therapy (IMRT) using the volume at risk approach (VARA): employing dose-volume histogram (DVH) and normal tissue complication probability (NTCP) to evaluate small bowel toxicity,” *Medical Dosimetry*, vol. 27, no. 2, pp. 121–129, 2002.
- [12] LÉTOURNEAU, D., WONG, J., OLDHAM, M., GULAM, M., WATT, L., JAFFRAY, D., SIEWERDSEN, J., and MARTINEZ, A., “Cone-beam-CT guided radiation therapy: technical implementation,” *Radiotherapy and Oncology*, vol. 75, no. 3, pp. 279–286, 2005.
- [13] LITTLE, D., DONG, L., LEVY, L., CHANDRA, A., and KUBAN, D., “Use of portal images and BAT ultrasonography to measure setup error and organ motion for prostate IMRT: implications for treatment margins,” *International Journal of Radiation Oncology Biology Physics*, vol. 56, no. 5, pp. 1218–1224, 2003.
- [14] MAGERAS, G. and YORKE, E., “Deep inspiration breath hold and respiratory gating strategies for reducing organ motion in radiation treatment\* 1,” in *Seminars in Radiation Oncology*, vol. 14, pp. 65–75, Elsevier, 2004.
- [15] OELFKE, U. and BORTFELD, T., “Inverse planning for x-ray rotation therapy: a general solution of the inverse problem,” *Physics in Medicine and Biology*, vol. 44, p. 1089, 1999.
- [16] RAMSEY, C., SCAPEROTH, D., ARWOOD, D., and OLIVER, A., “Clinical efficacy of respiratory gated conformal radiation therapy,” *Medical Dosimetry*, vol. 24, no. 2, pp. 115–119, 1999.
- [17] RUTT, B. and LEE, D., “The impact of field strength on image quality in MRI,” *Journal of Magnetic Resonance Imaging*, vol. 6, no. 1, pp. 57–62, 1996.
- [18] SCHENCK, J., JOLESZ, F., ROEMER, P., CLINE, H., LORENSEN, W., KIKINIS, R., SILVERMAN, S., HARDY, C., BARBER, W., and LASKARIS, E., “Superconducting open-configuration MR imaging system for image-guided therapy,” *Radiology*, vol. 195, no. 3, p. 805, 1995.
- [19] SCHIEPERS, C., PENNINGCKX, F., DE VADDER, N., MERCKX, E., MORTELMANS, L., BORMANS, G., MARCHAL, G., FILEZ, L., and AERTS, R., “Contribution of PET in the diagnosis of recurrent colorectal cancer: comparison with

- conventional imaging,” *European Journal of Surgical Oncology*, vol. 21, no. 5, pp. 517–522, 1995.
- [20] STROOM, J. and HEIJMEN, B., “Geometrical uncertainties, radiotherapy planning margins, and the ICRU-62 report,” *Radiotherapy and Oncology*, vol. 64, no. 1, pp. 75–83, 2002.
- [21] STRULAB, D., SANTIN, G., LAZARO, D., BRETON, V., and MOREL, C., “GATE (Geant4 Application for Tomographic Emission): a PET/SPECT general-purpose simulation platform,” *Nuclear Physics B-Proceedings Supplements*, vol. 125, pp. 75–79, 2003.
- [22] XING, L., LI, J., DONALDSON, S., LE, Q., and BOYER, A., “Optimization of importance factors in inverse planning,” *Physics in medicine and biology*, vol. 44, p. 2525, 1999.
- [23] XING, L., THORNDYKE, B., SCHREIBMANN, E., YANG, Y., LI, T., KIM, G., LUXTON, G., and KOONG, A., “Overview of image-guided radiation therapy,” *Medical Dosimetry*, vol. 31, no. 2, pp. 91–112, 2006.
- [24] ZHU, L., LEE, L., MA, Y., YE, Y., MAZZEO, R., and XING, L., “Using total-variation regularization for intensity modulated radiation therapy inverse planning with field-specific numbers of segments,” *Physics in medicine and biology*, vol. 53, p. 6653, 2008.